Supporting Information

Determination of the Structure and Dynamics of a Linear Polypeptide Gramicidin A at Atomic Scale Resolution

Bijay Laxmi Pradhan,[1,2] Prince Sen,[3] Adarsh Kumar,[3]Anirban Bhunia,[4] Krishna Kishor Dey,*[3] Manasi Ghosh*[2]

1. *Department of Physics, Institute of Science, Banaras Hindu University, Varanasi-221005, Uttar-Pradesh, India*
2. *Physics Section, Mahila Maha Vidyalaya, Banaras Hindu University, Varanasi-221005, Uttar-Pradesh, India*
3. *Department of Physics, Dr. Harisingh Gour Central University, Sagar-470003, Madhya-Pradesh, India*
4. *Department of Chemical Sciences, Bose Institute, Salt Lake, EN 80, Sector V, Kolkata 700091, West-Bengal, India*

*Corresponding authors: dey.krishna@gmail.com, manasi.ghosh@bhu.ac.in, manasi.ghosh@gmail.com

S1: Detail Description of the Solid and Liquid NMR Experiments

The ^{13}C 2DPASS CP-MAS SSNMR experiment enables correlation between the isotropic and anisotropic dimensions through a combination of shearing transformation and two-dimensional Fourier transformation. Overlapping resonances were resolved using the 2DPASS CP-MAS SSNMR technique, as differences in the CSA parameters of those resonance lines, whose isotropic chemical shift position is overlapped, provide clear separation. The CSA eigenvalues were determined from the sideband intensities observed in the spinning CSA sideband patterns corresponding to chemically distinct carbon sites. The 2DPASS CP-MAS SSNMR experiment employs five π pulses whose time evolution follows the PASS equation; however, the total duration of all PASS sequences remains constant. The experiment begins with a precisely calibrated 90° pulse on the ^{13}C nucleus (duration of the pulse is 3.3 μs), followed by a 15 s relaxation delay. 13-step Cogwheel phase cycling (COG13: 0, 1, 0, 1, 0, 1; 6) was implemented over 4030 scans, which is an integral multiple of 13.[1,2]The coherence transfer pathway used for this experiment was previously reported by Ghosh et al.[3] In the indirect dimension, sixteen data points were collected to account for the limited number of sidebands. The intensities of these sidebands, analysed using a graphical approach, were utilized to extract the CSA tensor. Finally, determination of the principal components of the CSA parameters was carried out using advanced computational tools such as HBA (http://anorganik.uni-

tuebingen.de/klaus/soft/index.php?p=hba/hba)[4] and RMN (www.physyapps.com/rmn-intuitive-signal-processing-physical-sciences).

Chemical shift anisotropy (CSA) interaction plays a crucial role in providing detailed information about molecular structure and dynamics. However, determining CSA parameters in static powder samples is often challenging due to issues like low sensitivity and significant spectral overlap. To overcome these limitations, several advanced methodologies have been introduced. These include two-dimensional MAS/CSA NMR experiments,[5] SUPER (Separation of Undistorted Powder Patterns by Effortless Recoupling),[6] ROCSA (Recoupling of Chemical Shift Anisotropy),[7] RNCSA (γ-encoded $R^{N^{v}}_{n}$-symmetry based chemical shift anisotropy),[8] as well as two-dimensional magic angle flipping (2DMAF),[9-11] magic angle turning (2DMAT),[12] and the phase-adjusted spinning sideband cross-polarization MAS approach (2DPASS CP-MAS) in solid-state NMR.[31,32] Many recoupling techniques determine CSA parameters by analysing spinning-sideband patterns or powder patterns. However, 2DPASS experiments are generally less effective for CSA measurements in strongly coupled systems because it cannot suppress homonuclear dipolar interactions efficiently. But we focus on ^{13}C nuclei at natural abundance (~1.1%), where homonuclear dipole-dipole interactions do not significantly influence the spinning sideband pattern. Despite this, decoupling heteronuclear dipolar interactions—especially the ^{1}H–^{13}C nuclei coupling—is essential for obtaining reliable data. To address this, we implement the SPINAL-64 decoupling sequence to extract CSA parameter. When performing the 2DPASS CP-MAS sequence, several potential sources of error must be considered, including improper optimization of the heteronuclear decoupling sequence, variations in MAS frequency, and temperature during the experiment. Addressing these issues is essential for accurate measurements of the CSA parameters. The 2DPASS method is widely applied to determine the principal components of CSA parameters across a range of systems, such as biopolymers,[33,13-17] active pharmaceutical ingredients of some drugs ,[34-36] glasses,[18] and charge-transfer cocrystals.[19]

The approach proposed by Torchia[37] for determining the spin-lattice relaxation time (T_1) of ^{13}C nuclei provides notable benefits. First of all, it enhances the sensitivity of low-γ ^{13}C signal through cross-polarization with high-γ ^{1}H spins. Consequently, it requires a much shorter relaxation delay—only about five times the ^{1}H relaxation time instead of that of ^{13}C—significantly reducing the overall experiment time compared to the conventional inversion recovery method for solids. However, the initial signal intensity obtained using the Torchia scheme is strongly influenced by the ^{1}H–^{13}C heteronuclear dipolar coupling constant (DCH) and the local proton density. Consequently, the system with fast motional dynamics can reduces DCH values, and those systems are not suitable for this technique. For this reason, the Torchia method is primarily applied to measure ^{13}C T_1 in rigid solids.[20]

All the liquid state NMR spectra of Gramicidin A were acquired using Bruker Advance NEO 600MHz NMR Spectrometer at SATHI-BHU, Central Discovery Centre, Banaras Hindu University. The samples for the liquid NMR were prepared by dissolving 20mg of gramicidin

A in 600µl DMSO-d6 solvent. The prepared sample was transferred to 5mm NMR tube and loaded in NMR spectrometer.

The 1H-15N HSQC experiment was carried out in BRUKER Avance neo spectrometer. 2,048 points were acquired over 0.12 s acquisition time in the direct dimension, and 256 points were acquired over 0.005 s acquisition time in the indirect dimension. 8 scans were averaged per increment. A recycle delay of 2 s was employed.

In 1H-13C HSQC experiment, 2048 points were acquired over 0.13 s acquisition time in the direct dimension, and 256 points were acquired over 0.005 s acquisition time in the indirect dimension. 16 scans were averaged per increment. A recycle delay of 2 s was employed.

In 1H-1H NOESY experiment 2,048 points were acquired over 0.13 s acquisition time in the direct dimension, and 256 points were acquired over 0.016 s acquisition time in the indirect dimension. 4 scans were averaged per increment. A recycle delay of 2 s was employed.

In 1H-13C HMBC experiment 4096 points were acquired over 0.27 s acquisition time in the direct dimension, and 128 points were acquired over 0.0019 s acquisition time in the indirect dimension. 16 scans were averaged per increment. A recycle delay of 2 s was employed.

In 1H-1H TCOSY experiment 2,048 points were acquired over 0.13 s acquisition time in the direct dimension, and 256 points were acquired over 0.016s acquisition time in the indirect dimension. 8 scans were averaged per increment. A recycle delay of 2 s was employed.

In 1H-1H COSY experiment 2,048 points were acquired over 0.13 s acquisition time in the direct dimension, and 128 points were acquired in the indirect dimension over 0.008 s acquisition time. 4 scans were averaged per increment. A recycle delay of 2 s was employed.

For COSY experiment we have used pulse program: cosygpppqf.[21,22] It generates a magnitude-mode spectrum with a quadrature detection in the F1 dimension.

HSQC pulse program name: hsqcedetgpsisp2.3. [23,24]

HMBC pulse program name: hmbcgplpndqf.[25,26,27]

NOESY pulse program: noesygpphpp.[28,29]

Table S1: The assignment of ^{13}C resonance lines by following 2D NMR correlation experiments like 2D ^{1}H-^{13}C HSQC, 2D ^{1}H-^{15}N HSQC, ^{1}H-^{13}C HMBC, ^{1}H-^{1}H COSY, and ^{1}H-^{1}H TOCSY and compared with previously published research article by Hawkes et al.[30]

^{13}C Nuclei	Isotropic Chemical Shift according to G.E. Hawkes and coauthors {Hawkes, G. H.; Lian, L. Y.; Randall, E. W.; Sales, K. D.; Curzon, E. H. The conformation of gramicidin A in dimethylsulphoxide solution: A full analysis of the one-and	Isotropic Chemical Shift according to current assignment by 2D NMR correlation experiments (ppm)

	two-dimensional ^{1}H, ^{13}C, and ^{15}N nuclear-magnetic-resonance spectra. *Eur. J. Biochem.*, **1987**, *166*(2), 437-445. } (ppm)	
C1	161.18	161.66
C2	56.49	56.83
C3	30.37	30.83
C4	19.34 or 19.29 or 19.22	19.77
C5	17.60 or 17.89 or 17.83	18.21
C6	171.01	171.50
C7	41.96	42.31
C8	168.45	168.96
C9	48.60	49.00
C10	18.16	18.62
C11	172.14	172.64
C12	51.34	51.68
C13	40.63	41.04
C14	24.31	24.71
C15	23.03	23.03
C16	21.34	21.72
C17	171.70	172.19
C18	48.69	49.08
C19	18.35	18.81
C20	172.26	172.77
C21	58.06 or 57.61	58.37
C22	30.74 or 30. 49	31.21
C23	19.34 or 19.29 or 19.22	19.73
C24	17.60 or 17.89 or 17.83	18.01
C25	171.01	171.50
C26	58.06 or 57.61	58.12
C27	30.74 or 30. 49	30.96
C28	19.34 or 19.29 or 19.22	19.66
C29	17.60 or 17.89 or 17.83	17.99
C30	171.01	171.50
C31	57.78	57.93
C32	30.30	30.74
C33	19.06	19.48
C34	17.60	18.31
C35	170.79	171.27
C36	53.93	54.27
C37	27.65 or 27.85	28.31
C38		110.18
C39		124.37
C40		136.57
C41		111.64
C42		121.19
C43		118.58

C44		118.83
C45		127.60
C46	171.29 or 171.3	171.79
C47	51.55	51.95
C48	40.49 or 40.36	40.78
C49	23.62	24.08
C50	22.57	22.99
C51	21.88 or 21.67 or 21.58	22.34
C52	171.76	172.25
C53	53.81	54.19
C54	27.65 or 27.85	28.06
C55		110.18
C56		124.28
C57		136.57
C58		111.64
C59		121.19
C60		118.58
C61		118.74
C62		127.60
C63	171.18 or 171.2	171.66
C64	51.55	51.91
C65	40.49 or 40.36	40.53
C66	23.62	23.99
C67	22.57	22.96
C68	21.88 or 21.67 or 21.58	22.13
C69	171.86	172.34
C70	54.02	54.36
C71	27.65 or 27.85	28.31
C72		110.72
C73		124.23
C74		136.57
C75		111.64
C76		121.19
C77		118.58
C78		118.74
C79		127.60
C80	171.62 or 171.5	172.13
C81	51.74	52.13
C82	40.49 or 40.36	40.90
C83	23.62	23.48
C84	22.57	22.95
C85	21.88 or 21.67 or 21.58	22.01
C86	171.70	172.19
C87	53.81	54.19
C88	27.65 or 27.85	28.06
C89		110.02
C90		124.23
C91		136.57

C92		111.64
C93		121.19
C94		118.58
C95		118.83
C96		127.60
C97	171.44 or 171.3	171.95
C98	41.78	42.17
C99	59.82	60.21

Table S2: The assignment of ^{1}H resonance lines by following 2D NMR correlation experiments like 2D ^{1}H-^{13}C HSQC, 2D ^{1}H-^{15}N HSQC, ^{1}H-^{13}C HMBC, ^{1}H-^{1}H COSY, and ^{1}H-^{1}H TOCSY and compared with previously published research article by Hawkes et al.[30]

^{1}H nuclei	Isotropic Chemical Shift according to G.E. Hawkes and coauthors { Hawkes, G. H.; Lian, L. Y.; Randall, E. W.; Sales, K. D.; Curzon, E. H. The conformation of gramicidin A in dimethylsulphoxide solution: A full analysis of the one-and two-dimensional ^{1}H, ^{13}C, and ^{15}N nuclear-magnetic-resonance spectra. *Eur. J. Biochem.*, **1987**, *166*(2), 437-445. } (ppm)	Isotropic Chemical Shift according to current assignment by 2D NMR correlation experiments (ppm)
H1	8.10	8.05
H2	3.47	4.22-4.26
H3	2.03	1.81
H4A, H4B, H4C	0.87	0.78-0.82
H5A, H5B, H5C	0.87	0.57-0.59
H7A, H7B	3.78	3.72
H9		4.27-4.32
H10A, H10B, H10C	1.24	1.20
H12	4.31	4.22-4.26
H13A, H13B	1.53	1.46
H14	1.63	1.56
H15A, H15B, H15C	0.84	0.65

H16A,H16B, H16C	0.84	0.78-0.82
H18		4.46-4.58
H19A, H19B, H19C	1.26	1.20
H21		4.27-4.32
H22	2.06	1.95-2.03
H23A, H23B, H23C	0.88	0.57-0.59
H24A, H24B, H24C	0.88	0.78-0.82
H26		4.27-4.32
H27	2.06	1.95-2.03
H28A, H28B, H28C	0.88	0.83-0.87
H29A, H29B, H29C	0.88	0.50-0.52
H31	4.21	4.12-4.19
H32	1.93	1.95-2.03
H33A, H33B, H33C	0.64-0.69	0.57-0.59
H34A, H34B, H34C	0.64-0.69	0.83-0.87
H36		4.61-4.71
H37A	3.25	3.11-3.23
H37B	2.9	2.91
H39		7.08-7.09
H41		7.28-7.31
H42		7.01-7.05
H43		6.91-6.97
H44		7.57-7.58
H47	4.20	4.12-4.19
H48A H48B	1.25	1.11
H49	0.91-0.99	0.97
H50A, H50B, H50C	0.61-0.68	0.50-0.52
H51A, H51B, H51C	0.61-0.68	0.57-0.59
H53		4.46-4.58
H54A	3.25	3.25
H54B	2.9	2.91
H56		7.08-7.09
H58		7.28-7.31
H59		7.01-7.05
H60		6.91-6.97
H61		7.53-7.54

H64	4.22	4.22-4.26
H65A, H65B	1.17	1.11
H66	0.91-0.99	0.97
H67A, H67B, H67C	0.61-0.68	0.65
H68A, H68B, H68C	0.61-0.68	0.57-0.59
H70		4.61-4.71
H71A	3.25	3.11-3.23
H71B	2.9	2.91
H73		7.08-7.09
H75		7.28-7.31
H76		7.01-7.05
H77		6.91-6.97
H78		7.57-7.58
H81	4.18	4.12-4.19
H82A, H82B	1.17	1.11
H83	0.91-0.99	0.97
H84A, H84B, H84C	0.61-0.68	0.83-0.87
H85A, H85B, H85C	0.61-0.68	0.50-0.52
H87		4.46-4.58
H88A	3.11-3.23	3.28
H88B	2.9	2.91
H90		7.08-7.09
H92		7.28-7.31
H93		7.01-7.05
H94		6.91-6.97
H95		7.53-7.54
H98A, H98B	3.11-3.23	3.25
H99A, H99B	3.43	3.47
$H1_N$	8.18	8.19-8.23
$H2_N$	8.30	8.28-8.31
$H3_N$	7.99	7.98-7.99
$H4_N$	8.10	8.11-8.14
$H5_N$	7.94	7.92-7.94
$H6_N$	7.78	7.73-7.74
$H7_N$	7.98	7.92-7.94
$H8_N$	7.89	7.77-7.78
$H9_N$	8.13	8.19-8.23
$H10_N$		10.76
$H11_N$	7.99	8.02-8.03
$H12_N$	8.20	8.19-8.23

$H13_N$		10.71
$H14_N$	7.99	8.02-8.03
$H15_N$	8.20	8.19-8.23
$H16_N$		10.76
$H17_N$	8.11-8.14	8.08
$H18_N$	8.25	8.28-8.31
$H19_N$		10.71
$H20_N$	7.83	7.92-7.94
$H17_O$		4.61-4.71

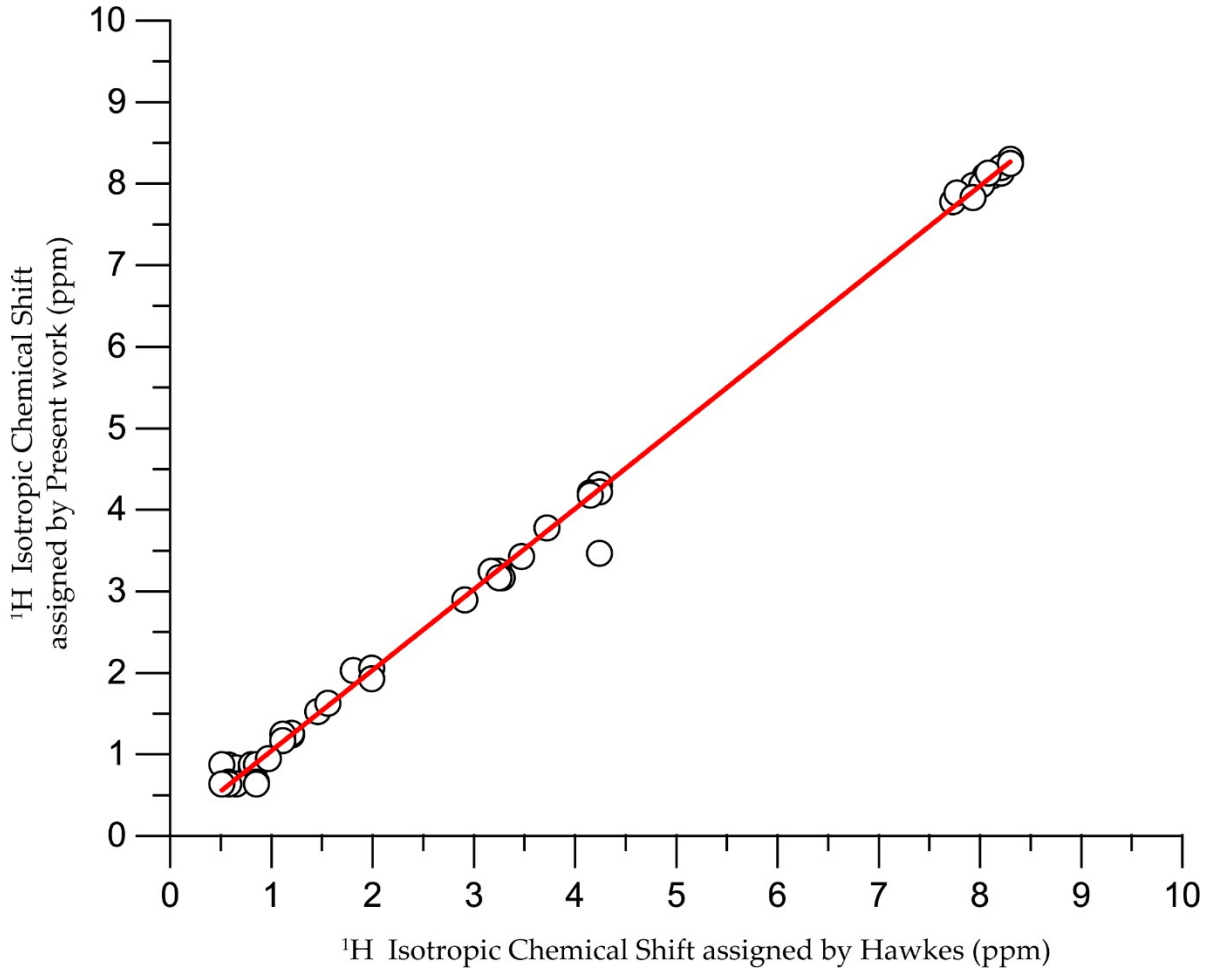

Figure S1: We compared our ^{1}H chemical-shift assignments with those reported in the previously published study by G. E. Hawkes and coauthors.[30] The isotropic chemical shifts assigned to each ^{1}H nucleus show excellent agreement with the earlier work, exhibiting a linear correlation.

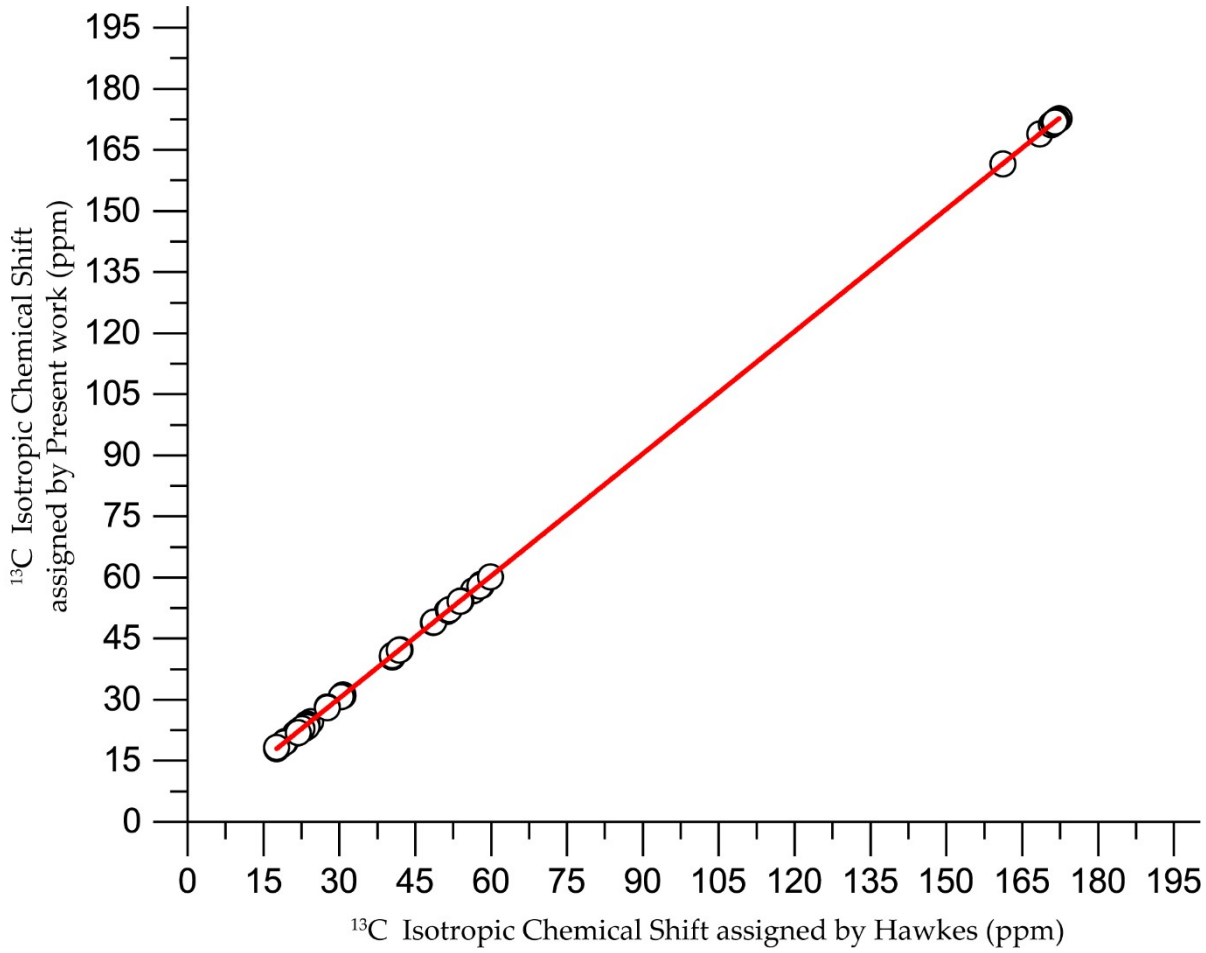

Figure S2: We compared our ^{13}C chemical-shift assignments with those reported in the previously published study by G. E. Hawkes and coauthors.[30] The isotropic chemical shifts assigned to each ^{13}C nucleus show excellent agreement with the earlier work, exhibiting a linear correlation.

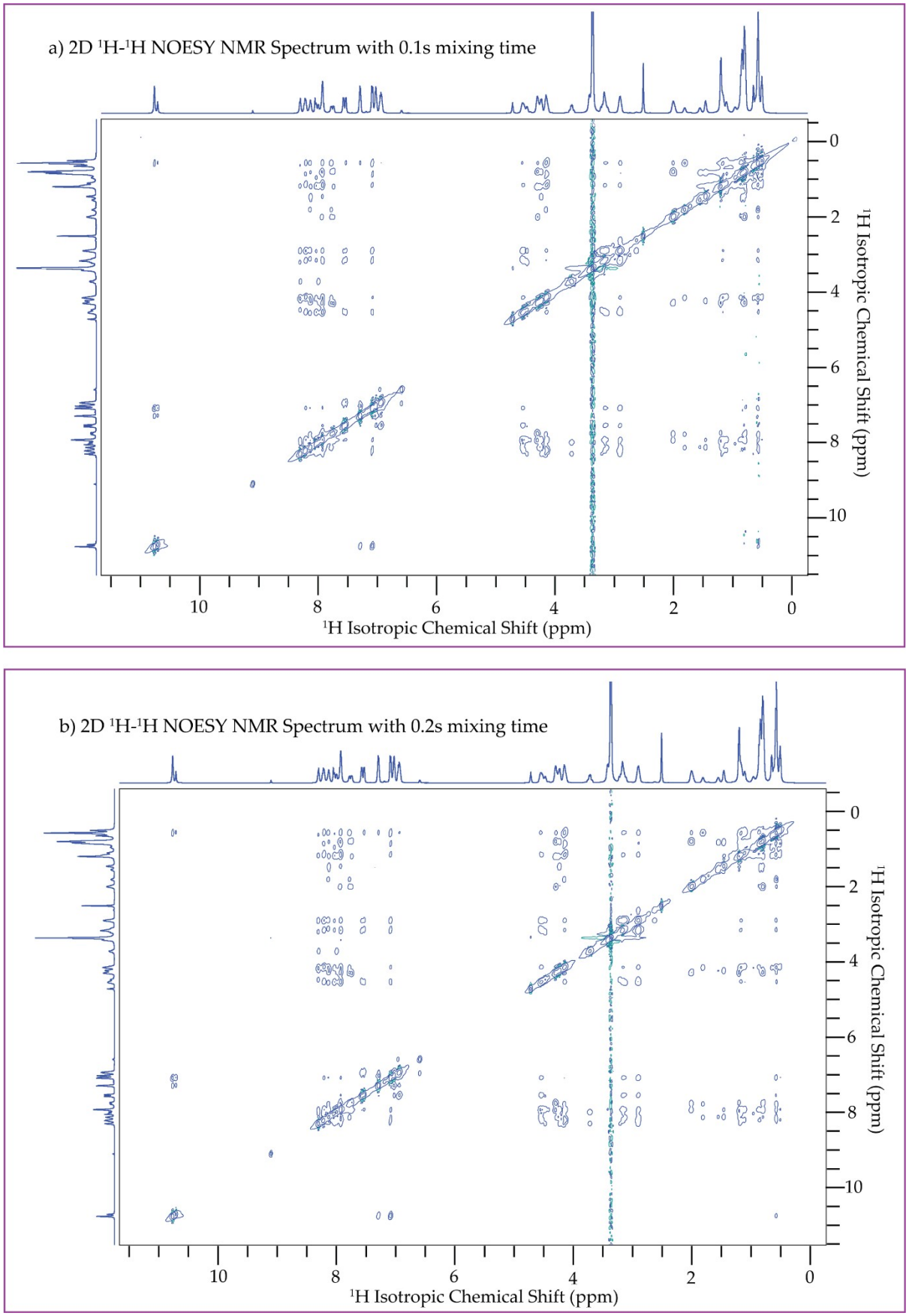

Figure S3: ^{1}H-^{1}H NOESY spectrum at mixing time (a) 0.1 s , and (b) 0.2 s.

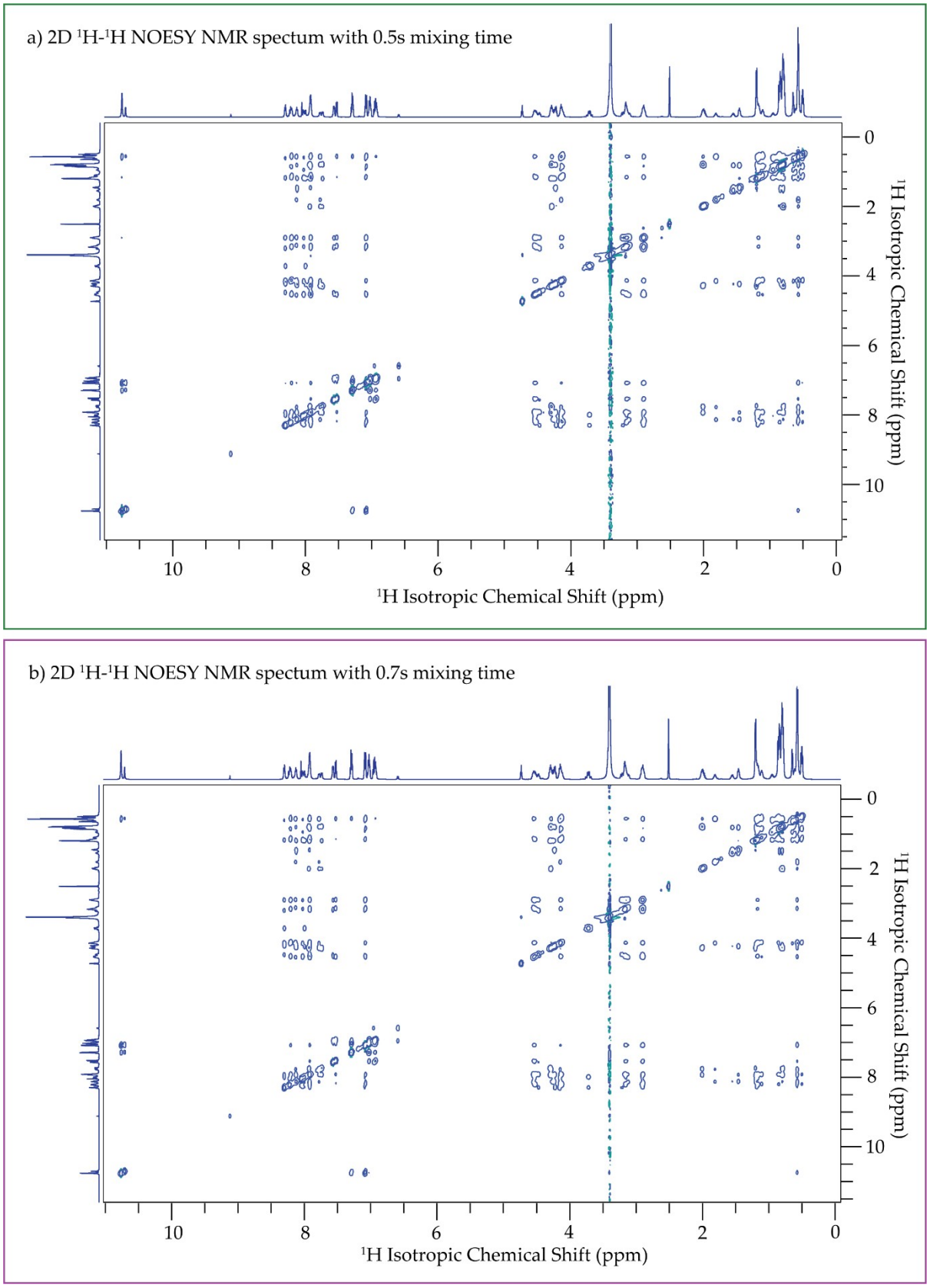

Figure S4: ^{1}H-^{1}H NOESY spectrum at mixing time (a) 0.5 s , and (b) 0.7 s.

The final assignment of proton resonances provides detailed insights into the chemical environments of various protons in different amino acid residues of gramicidin A. Methyl group protons, except for those in the L-alanine residues, exhibit chemical shift values in the range of 0.50 ppm to 0.87 ppm. In contrast, the methyl protons of the L-alanine groups display a comparatively less shielded shift at 1.20 ppm, indicating a slightly more deshielded environment. Protons H49, H83 and H66, located on leucine residues, exhibit a characteristic chemical shift of 0.97 ppm and appear as a nonet in the ^{1}H NMR spectrum. Similarly, the methylene protons H48A, H48B, H82A, H82B, H65A, and H65B in D-leucine residues, are assigned to a slightly more less shielded region at approximately 1.10 ppm. Notably, the methylene protons H13A and H13B show a chemical shift of 1.46 ppm, which is relatively less shielded compared to similar protons in other leucine residues. Protons attached to carbons adjacent to methyl groups in valine and leucine residues appear in the range of 1.56 to 2.03 ppm. For tryptophan residues, protons attached to carbons C37, C71, C88, and C54 exhibit chemical shifts between 2.91 to 3.23 ppm. On the other hand, those protons bonded to carbons in ethanolamine amino acid resonate between 3.20 ppm to 3.43 ppm. Glycine methylene protons H7A and H7B are observed at 3.72 ppm. The aromatic protons located within the indole rings of tryptophan residues appear further less shielded, with chemical shift values ranging between 6.91 to 7.58 ppm, due to the presence of $\pi -$ electron-rich aromatic ring.

Table S3: Assignment of Isotropic Chemical Shift values^{1}H nuclei in gramicidin A

Isotropic Chemical Shift of ^{1}H nuclei (δ_{iso}) (ppm)	^{1}H Nuclei
0.50-0.52	H50A, H50B, H50C, H85A, H85B, H85C, H29A, H29B, H29C
0.57-0.59	H33A, H33B, H33C, H23A, H23B, H23C, H51A, H51B, H51C, H68A, H68B, H68C, H5A, H5B, H5C
0.65	H15A, H15B, H15C, H67A, H67B, H67C
0.78-0.82	H24A, H24B, H24C, H4A, H4B, H4C, H16A, H16B, H16C
0.83-0.87	H28A, H28B, H28C, H84A, H84B, H84C, H34A, H34B, H34C
0.97	H83, H49, H66
1.11	H48A, H48B, H65A, H65B, H82A, H82B
1.20	H19A, H19B, H19C, H10A, H10B, H10C
1.46	H13A, H13B
1.56	H14
1.81	H3
1.95-2.03	H32, H27, H22
2.50	solvent
2.91	H37B, H54B, H71B, H88B
3.11-3.23	H88A, H98A, H98B, H37A, H54A, H71A
3.43	H99A, H99B

3.72	H7A, H7B
4.12-4.19	H47, H81, H31
4.22-4.26	H12, H2, H64
4.27-4.32	H9, H26, H21
4.46-4.58	H87, H18, H53
4.61-4.71	H36, H70, $H17_O$
6.91-6.97	H94, H60, H77, H43
7.01-7.05	H93, H59, H76, H42
7.08-7.09	H90, H56, H73, H39
7.28-7.31	H58, H92, H41, H75
7.53-7.54	H61, H95
7.57-7.58	H78, H44
7.73-7.74	$H6_N$
7.77-7.78	$H8_N$
7.92-7.94	$H7_N$, $H20_N$, $H5_N$
7.98-7.99	$H3_N$
8.02-8.03	$H11_N$, $H14_N$
8.05	H1
8.11-8.14	$H4_N$, $H17_N$
8.19-8.23	$H12_N$, $H15_N$, $H1_N$, $H9_N$
8.28-8.31	$H2_N$, $H18_N$
10.71	$H13_N$, $H19_N$
10.76	$H10_N$, $H16_N$

Table S4: Assignment of ^{13}C isotropic chemical shift values of gramicidin A.

Isotropic Chemical Shift (ppm)	^{13}C nuclei
17.987	C29
18.013	C24
18.211	C5
18.313	C34
18.622	C10
18.812	C19
19.479	C33
19.662	C28
19.727	C23
19.771	C4
21.717	C16
22.009	C85
22.133	C68
22.344	C51
22.951	C84
22.964	C67
22.997	C50
23.028	C15
23.483	C83
23.996	C66

24.080	C49
24.710	C14
28.062	C54, C88
28.306	C37, C71
30.743	C32
30.830	C3
30.964	C27
31.215	C22
40.532	C65
40.784	C48
40.897	C82
41.038	C13
42.168	C98
42.308	C7
49.005	C9
49.078	C18
51.676	C12
51.910	C64
51.954	C47
52.135	C81
54.189	C53, C87
54.266	C36
54.357	C70
56.834	C2
57.933	C31
58.120	C26
58.368	C21
60.212	C99
110.02	C89
110.18	C38, C55
110.72	C72
111.64	C41, C58, C75, C92
118.58	C43, C60, C77, C94
118.74	C61, C78
118.83	C44, C95
121.19	C42, C59, C76, C93
124.23	C73, C90
124.28	C56
124.37	C39
127.60	C45, C62, C79, C96
136.57	C57, C40, C74, C91
161.66	C1
168.96	C8
171.27	C35
171.50	C30, C6, C25
171.665	C63
171.791	C46

171.951	C97
172.134	C80
172.197	C17, C86
172.248	C52
172.34	C69
172.643	C11
172.775	C20

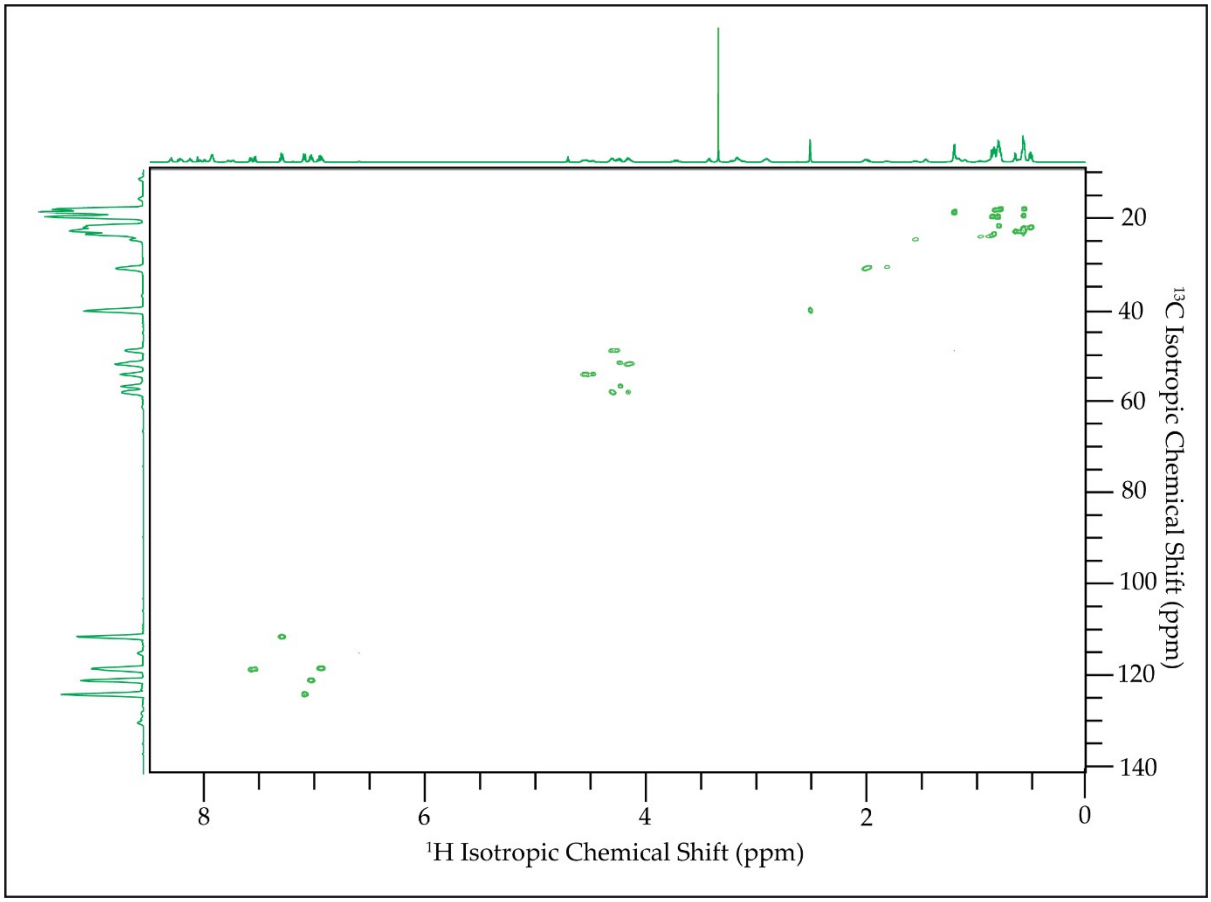

Figure S5: 2D ^{1}H-^{13}C HSQC spectrum of gramicidin A.

Table S5: Assignment of 2D ^{1}H-^{13}C HSQC NMR spectrum of gramicidin A

Isotropic Chemical Shift of ^{1}H nuclei (ppm)	^{1}H Nuclei	Isotropic Chemical Shift of ^{13}C nuclei (ppm)	^{13}C Nuclei correlated through 2D ^{1}H-^{13}C HSQC NMR experiment
7.574	H78	118.74	C78
7.532	H61	118.74	C61
7.292	H58, H92, H41, H75	111.64	C41, C58, C75, C92
7.087	H90, H56, H73, H39	124.23	C73, C90
		124.28	C56
		124.37	C39
7.027	H93, H59, H76, H42	121.2	C42, C59, C76, C93

6.934	H94, H60, H77, H43	118.53	C43, C60, C77, C94
4.47	H87	54.189	C87, C53
4.54	H53		
4.289	H9	49.06	C9
4.297	H26	57.93	C26
4.234	H12	51.63	C12
4.227	H2	56.87	C2
4.152	H47, H81	52.01	C47, C81
4.158	H31	58.12	C31
1.99	H27	30.96	C27
1.82	H3	30.83	C3
1.557	H14	24.71	C14
1.204	H19A, H19B, H19C,	18.69	C10
	H10A, H10B, H10C	18.81	C19
0.968	H49, H66	23.996	C66
		24.080	C49
0.862	H28A, H28B, H28C	19.662	C28
0.844	H84A, H84B, H84C	23.48	C84
0.839	H34A, H34B, H34C	18.3	C34
0.81	H4A, H4B, H4C	19.771	C4
0.805	H16A, H16B, H16C	21.74	C16
0.785	H24A, H24B, H24C	18.09	C24
0.654	H15A, H15B, H15C	23.02	C15
0.57	H29A, H29B, H29C	18.01	C29
0.579	H33A, H33B, H33C	19.479	C33
0.577	H51A, H51B, H51C	22.34	C51
0.503-0.519	H85A, H85B, H85C	22.06	C85

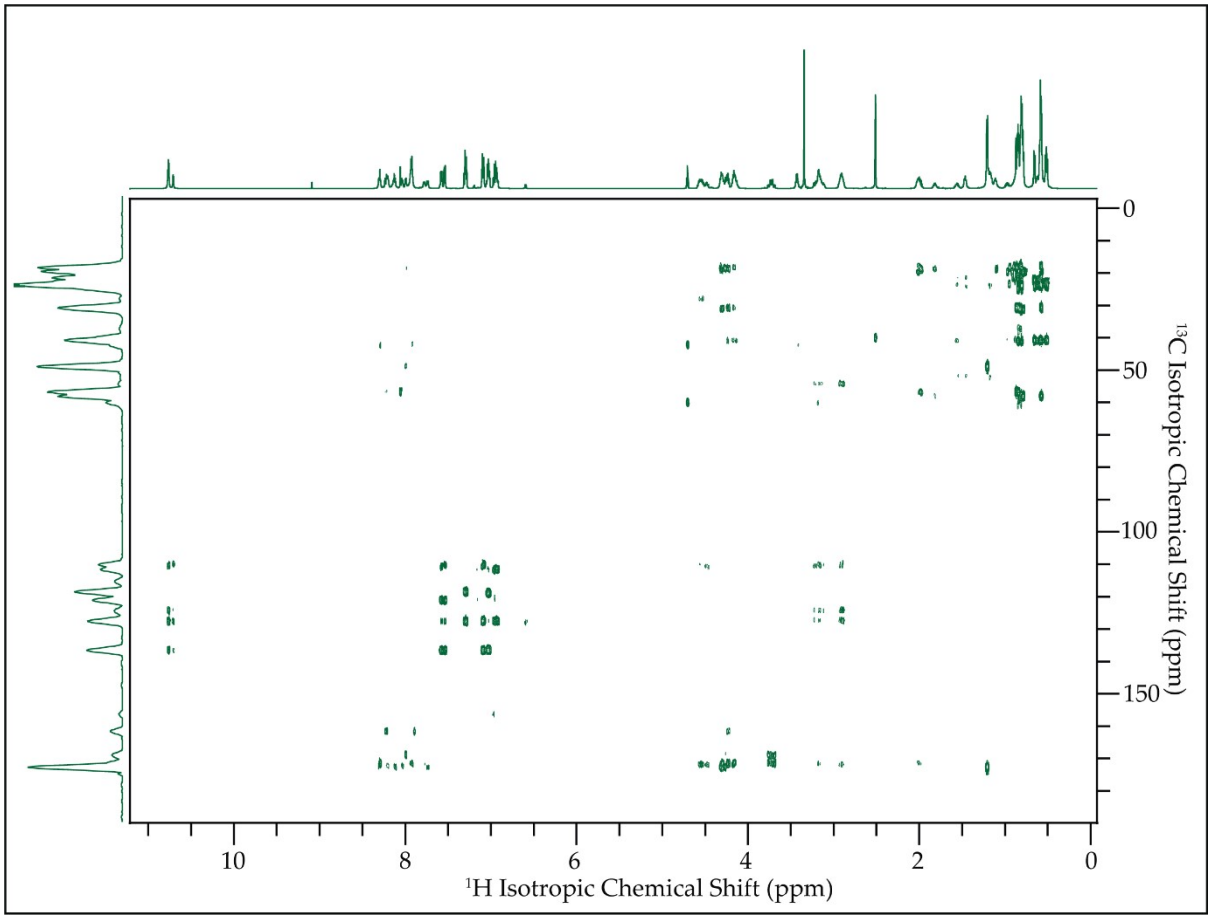

Figure S6: 2D ^{1}H-^{13}C HMBC NMR spectrum of gramicidin A.

Table S6: Assignment of 2D ^{1}H-^{13}C HMBC NMR spectrum of gramicidin A

^{1}H Isotropic Chemical Shift (ppm)	^{1}H Nuclei	^{13}C Isotropic Chemical Shift (ppm)	^{13}C Nuclei connected through HMBC NMR experiment
10.76	$H10_N$, $H16_N$	110.18 124.37 127.60 136.57	C38 C39 C45, C79 C40, C74
10.71	$H13_N$, $H19_N$	110.18 124.23 124.37 127.60 136.57	C55 C90 C56 C62, C96 C57, C91
8.05	H1	56.83	C2
8.29	$H2_N$	42.31	C7
7.99	$H3_N$	49.01	C9
7.92	$H20_N$	42.17	C98
7.99	$H3_N$	18.81	C19
8.29	$H2_N$	171.50	C6
8.22	$H1_N$	161.66	C1

8.20	$H15_N$	172.34	C69
7.99	$H3_N$	168.96	C8
7.92	$H7_N$	171.50	C30
7.77	$H8_N$	171.50	C30
7.73	$H6_N$	172.77	C20
7.57	H78, H44	110.72 121.19 127.60 136.57	C72 C42, C76 C45, C79 C40, C74
7.54	H61, H95	110.18 121.19 127.60 136.57	C55 C59, C93 C62, C96 C57, C91
7.29	H58, H92, H41, H75	118.58 127.60	C43, C60, C77, C94 C45, C62, C79, C96
7.084	H90, H56, H73, H39	110.18 127.60 136.57	C38, C55 C45, C62, C79, C96 C57, C40, C74, C91
7.032	H93, H59, H76, H42	118.74 136.57	C61, C78 C57, C40, C74, C91
6.948	H94, H60, H77, H43	111.64	C41, C58, C75, C92
4.7	$H17_O$	42.17 60.21	C98 C99
4.55	H87	28.06 110.02 171.95	C88 C89 C97
4.31	H9, H21	18.62 31.21 172.77	C10 C22 C20
4.28	H26, H21	171.50	C25
4.26	H12	172.64	C11
4.24	H2	171.50 161.66	C6 C1
4.22	H64	171.63	C63
4.16	H47	171.79	C46
3.72	H7A, H7B	168.96 171.50	C8 C6
4.54	H87	28.06	C88
4.30	H21	31.21 18.81	C22 C19
4.26	H9	18.62	C10
4.23	H64	40.78	C65
4.16	H81, H31	18.31 30.74 40.89	C34 C32 C82
3.41	H99A, H99B	42.17	C98
3.22	H88A, H54A	54.19	C53, C87
3.20	H71A	54.36	C70
3.18	H98A, H98B	60.21	C99

2.90	H54B, H88B	54.19	C53, C87
3.20	H88A, H37A, H54A, H71A	110.72 124.23 127.60	C72 C73, C90 C45, C62, C79, C96
2.90	H37B, H54B	110.18	C38, C55
3.177	H54A	171.66	C63
2.90	H88B	171.95	C97
2.015	H27	19.66	C28
1.99	H22	18.01	C24
1.20	H19A, H19B, H19C	172.77 18.81	C20 C19
1.20	H10A, H10B, H10C	49.01	C9
0.97	H83	23.48	C83
0.85	H34A, H34B, H34C	19.48 30.74	C33 C32
0.81	H4A, H4B, H4C	18.21	C5
0.79	H24A, H24B, H24C	19.72	C23
0.80	H67A, H67B, H67C	23.99	C66
0.83	H28A, H28B, H28C	30.96	C27
0.80	H24A, H24B, H24C	31.21	C22
0.84	H84A, H84B, H84C	40.89	C82
0.80	H16A, H16B, H16C	41.04	C13
0.84	H34A, H34B, H34C	57.93	C31
0.78	H24A, H24B, H24C	58.12	C26
0.65	H67A, H67B, H67C	22.13 23.99	C68 C66
0.65	H15A, H15B, H15C	41.04	C13
0.57	H51A, H51B, H51C, H33A, H33B, H33C, H23A, H23B, H23C, H68A, H68B, H68C	18.01 23.99 30.74 40.53 57.93	C24 C66 C32 C48 C31
0.52	H50A. H50B, H50C, H85A, H85B, H85C	23.48 40.53	C83 C48

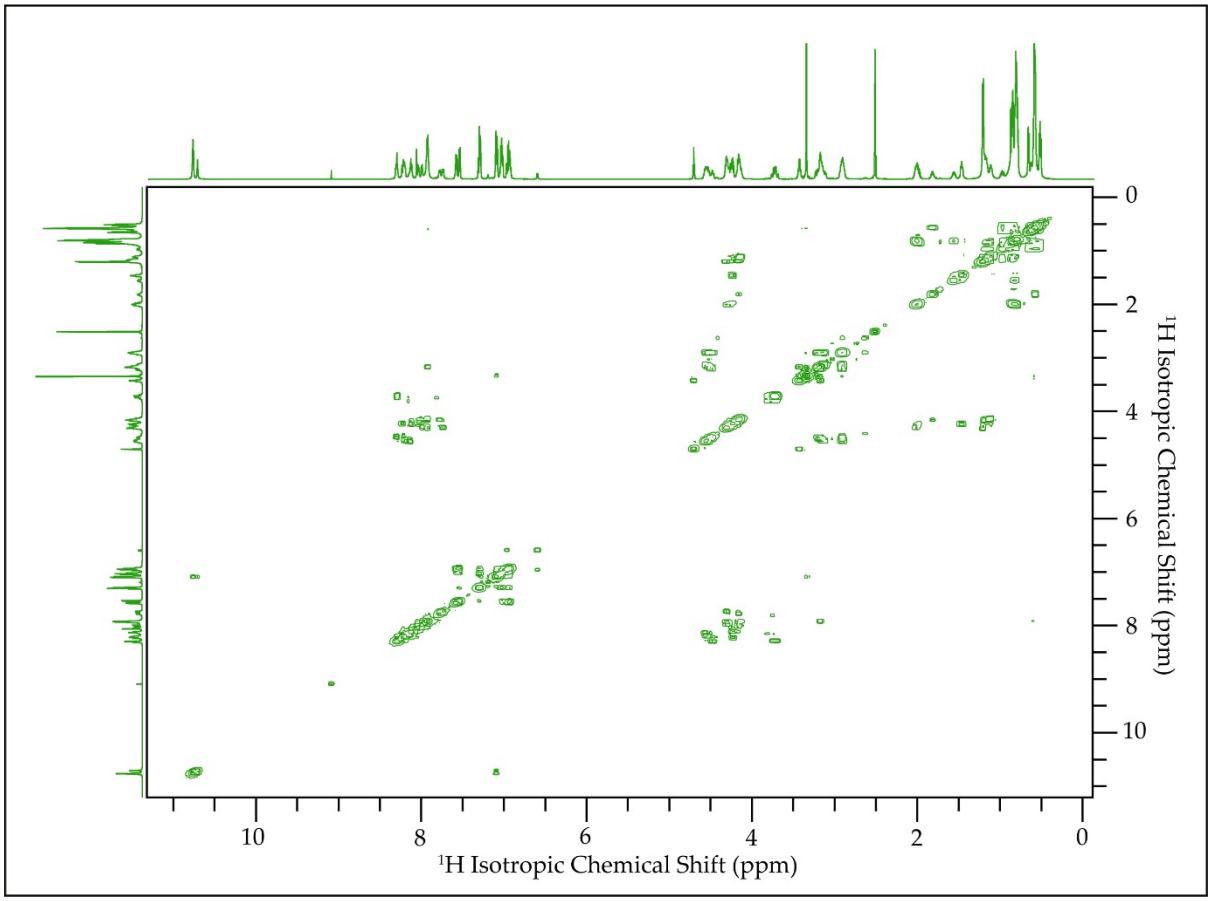

Figure S7: 2D ^{1}H-^{1}H COSY spectrum of gramicidin A.

Table S7: Assignment of ^{1}H-^{1}H COSY NMR spectrum of gramicidin A.

^{1}H Isotropic Chemical Shift (ppm)	^{1}H nuclei	^{1}H Isotropic Chemical Shift (ppm)	Correlated ^{1}H nuclei through COSY experiment
10.76	$H10_N$, $H16_N$	7.09	H39, H73
10.71	$H13_N$, $H19_N$	7.09	H56, H90
8.30	$H18_N$	4.47	H87
8.29	$H2_N$	3.72	H7A, H7B
8.23	$H1_N$	4.23	H2
8.20	$H12_N$	4.55	H53
8.12	$H4_N$	4.24	H12
8.02	$H11_N$	4.17	H47
8.03	$H14_N$	4.24	H64
7.98	$H3_N$	4.29	H9
7.93	$H7_N$	4.30 4.13	H26 H31
7.92	$H20_N$	3.16	H98A, H98B
7.77	$H8_N$	4.16	H31
7.74	$H6_N$	4.30	H21
7.57	H78,	6.93	H77,

	H44		H43
7.29	H58, H92, H41, H75	7.02	H59, H93, H42, H76
4.69	$H17_O$	3.43	H99A, H99B
4.49	H87, H53	2.91 3.20	H88B, H54B H88A, H54A
4.27	H9	1.20	H10A, H10B, H10C
4.31	H26	2.01	H27
4.25	H12	1.46	H13A, H13B
4.15	H47, H81	1.11	H48A, H48B H82A, H82B
1.99	H22	0.81	H24A, H24B, H24C
1.81	H3	0.57	H5A, H5B, H5C
0.97	H49	0.58	H51A, H51B, H51C
0.79	H16A, H16B, H16C	0.65	H15A, H15B, H15C

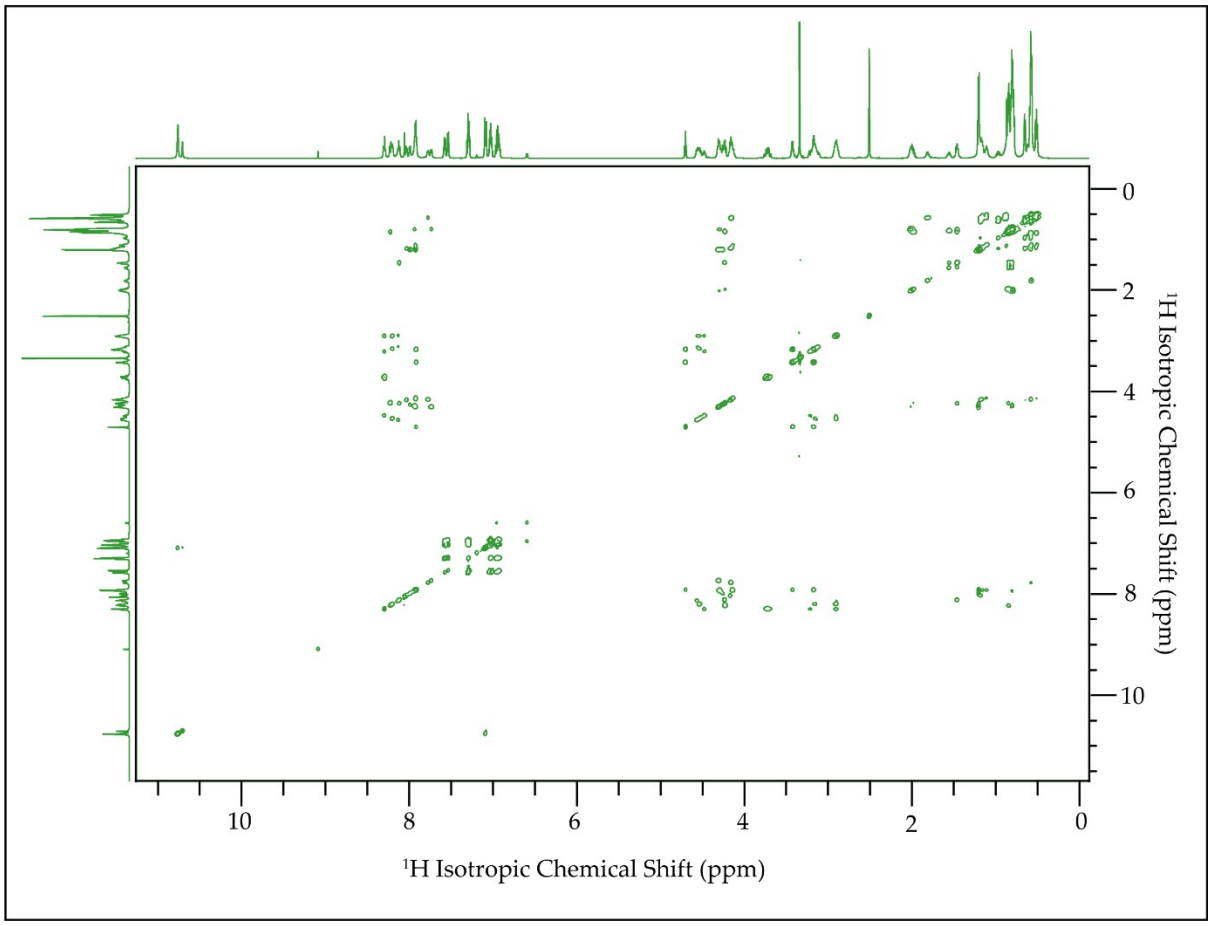

Figure S8: 2D ^{1}H-^{1}H TOCSY NMR spectrum of gramicidin A.

Table S8: Assignment of 2D ^{1}H-^{1}H TOCSY NMR spectrum of gramicidin A

^{1}H Isotropic Chemical Shift (ppm)	^{1}H nuclei	^{1}H Isotropic Chemical Shift (ppm)	^{1}H nuclei interacted thorough TOCSY experiment
10.76	$H10_N$, $H16_N$	7.09	H39, H73
10.71	$H13_N$, $N19_N$	7.08	H56, H90
8.29	$H18_N$, $H2_N$	2.91	H88B
		3.21	H88A, H98A, H98B
		3.72	H7A, H7B
		4.47	H87
8.23	$H9_N$	0.85	H34A, H34B, H34C
		1.98	H32
8.20	$H12_N$, $H15_N$, $H9_N$	2.91	H54B, H71B, H37B
		3.15	H54A, H71A, H37A
		4.54	H53
8.23	$H1_N$, $H15_N$	4.23	H64, H2
8.13	$H17_N$	2.91	H71B
		3.12	H71A
8.12	$H4_N$	4.56	H18
		4.22	H12
		1.46	H13A, H13B
		0.81	H16A, H16B, H16C
		1.19	H10A, H10B, H10C
8.03	$H11_N$, $H14_N$	0.58	H51A, H51B, H51C, H68A, H68B, H68C
		0.65	H67A, H67B, H67C
		1.11	H65A, H65B
		4.16	H47
7.99	$H3_N$	1.20	H10A, H10B, H10C
		4.26	H12
7.93	$H7_N$	4.29	H26, H21
		2.01	H27, H22
		0.79	H24A, H24B, H24C
7.92	$H20_N$, $H7_N$, $H5_N$	0.52	H29A, H29B, H29C
		0.58	H23A, H23B, H23C
		3.16	H88A, H98A, H98B
		3.43	H99A, H99B
		4.26	H12
		4.71	$H17_O$
7.78	$H8_N$	0.58	H33A, H33B, H33C
		4.15	H31
7.73	$H6_N$	4.31	H21
		2.01	H22
		0.80	H24A, H24B, H24C
7.09	H90, H56, H73, H39	2.91	H37B, H54B, H71B, H88B
8.22	H1N	8.05	H1
7.57	H78, H44	7.29	H41, H75

7.53	H61, H95	7.29	H58, H92
7.04	H93, H59, H76, H42	7.56 7.29	H78, H44 H58, H92, H41, H75
6.94	H94, H60, H77, H43	7.57 7.29	H78, H44 H58, H92, H41, H75
4.69	H36, H70, $H17_O$	3.17 3.43	H98A, H98B, H37A, H71A H99A, H99B
4.55	H87, H53	2.91 3.16	H54B, H88B H88A, H98A, H98B, H54A
4.29	H21, H26	0.80 2.01	H24A, H24B, H24C H27, H22
4.32	H9, H21	1.20	H19A, H19B, H19C, H10A, H10B, H10C
4.23	H12, H2	0.82 1.46	H4A, H4B, H4C, H16A, H16B, H16C H13A, H13B
4.15	H47, H31	0.58 0.97 0.89 1.17	H33A, H33B, H33C, H51A, H51B, H51C H83, H49 H84A, H84B, H84C H48A, H48B
3.43	H99A, H99B	3.17	H98A, H98B
2.01	H22	0.80	H24A, H24B, H24C
1.81	H3	0.57	H5A, H5B, H5C
1.46	H13A, H13B	1.56	H14
0.81	H16A, H16B, H16C	1.56 1.46	H14 H13A, H13B
1.11	H48A, H48B H65A, H65B	0.59 0.65	H51A, H51B, H51C H67A, H67B, H67C
0.65	H67A, H67B, H67C	1.11 0.97	H65A, H65B H66
0.58	H51A, H51B, H51C	1.11 0.97	H48A, H48B H83, H49
0.51	H50A, H50B, H50C, H29A, H29B, H29C, H85A, H85B, H85C	1.11 0.87	H48A, H48B, H65A H28A, H28B, H28C, H84A, H84B, H84C

Table S9: Assignment of 2D ^{1}H-^{1}H NOESY spectra of gramicidin A

^{1}H Isotropic Chemical Shift (ppm)	^{1}H Nuclei	^{1}H Isotropic Chemical Shift (ppm)	^{1}H Nuclei interacted through NOESY experiment

10.76	$H10_N$, $H16_N$	0.57	H33A, H33B, H33C, H23A, H23B, H23C, H51A, H51B, H51C, H68A, H68B, H68C, H5A, H5B, H5C
		7.09	H90, H56, H73, H39
		7.31	H58, H92, H41, H75
10.71	$H13_N$, $H19_N$	0.57	H33A, H33B, H33C, H23A, H23B, H23C, H51A, H51B, H51C, H68A, H68B, H68C, H5A, H5B, H5C
		7.09	H90, H56, H73, H39
		7.31	H58, H92, H41, H75
8.30	$H2_N$, $H18_N$	0.65	H15A, H15B, H15C, H67A, H67B, H67C
		1.11	H48A, H48B, H65A, H65B, H82A, H82B
		2.91	H37B, H54B, H71B, H88B
		3.23	H88A, H98A, H98B, H37A, H54A, H71A
		3.72	H7A, H7B
		4.17	H47, H81, H31
		4.47	H87, H18, H53
		7.94	$H7_N$, $H20_N$, $H5_N$
8.21	$H12_N$, $H15_N$, $H1_N$, $H9_N$	0.58	H33A, H33B, H33C, H23A, H23B, H23C, H51A, H51B, H51C, H68A, H68B, H68C, H5A, H5B, H5C
		0.87	H28A, H28B, H28C, H84A, H84B, H84C, H34A, H34B, H34C
		1.11	H48A, H48B, H65A, H65B, H82A, H82B
		2.91	H37B, H54B, H71B, H88B
		3.17	H88A, H98A, H98B, H37A, H54A, H71A
		4.15	H47, H81, H31
		4.54	H87, H18, H53
		7.09	H90, H56, H73, H39
8.13	H4N, H17N	0.59	H33A, H33B, H33C, H23A, H23B, H23C, H51A, H51B, H51C, H68A, H68B, H68C, H5A, H5B, H5C
		1.81	H3
		2.91	H37B, H54B, H71B, H88B
		3.12	H88A, H98A, H98B, H37A, H54A, H71A
		4.22	H12, H2, H64
		4.56	H87, H18, H53
8.03	H11N, H14N	0.59	H33A, H33B, H33C, H23A, H23B, H23C, H51A, H51B, H51C, H68A, H68B, H68C, H5A, H5B, H5C
		0.97	H83, H49, H66
		1.11	H48A, H48B, H65A, H65B, H82A, H82B

		2.91	H37B, H54B, H71B, H88B
		3.15	H88A, H98A, H98B, H37A, H54A, H71A
		4.15	H47, H81, H31
		4.56	H87, H18, H53
		7.08	H90, H56, H73, H39
7.78	H8N	0.59	H33A, H33B, H33C, H23A, H23B, H23C, H51A, H51B, H51C, H68A, H68B, H68C, H5A, H5B, H5C
		0.78	H24A, H24B, H24C, H4A, H4B, H4C, H16A, H16B, H16C
		1.81	H3
		2.01	H32, H27, H22
		4.29	H9, H26, H21
7.73	H6N	0.80	H24A, H24B, H24C, H4A, H4B, H4C, H16A, H16B, H16C
		1.11	H48A, H48B, H65A, H65B, H82A, H82B
		2.01	H32, H27, H22
		4.31	H9, H26, H21
7.57	H78, H44	2.91	H37B, H54B, H71B, H88B
		3.18	H88A, H98A, H98B,H37A, H54A, H71A
		4.53	H87, H18, H53
		6.95	H94, H60, H77, H43
7.54	H61, H95	0.57	H33A, H33B, H33C, H23A, H23B, H23C, H51A, H51B, H51C, H68A, H68B, H68C, H5A, H5B, H5C
		2.91	H37B, H54B, H71B, H88B
		3.14	H88A, H98A, H98B, H37A, H54A, H71A
		4.46	H87, H18, H53
		6.95	H94, H60, H77, H43
7.29	H58, H92, H41, H75	0.57	H33A, H33B, H33C, H23A, H23B, H23C, H51A, H51B, H51C, H68A, H68B, H68C, H5A, H5B, H5C
		7.03	H93, H59, H76, H42
7.08	H90, H56, H73, H39	0.57	H33A, H33B, H33C, H23A, H23B, H23C, H51A, H51B, H51C, H68A, H68B, H68C, H5A, H5B, H5C
		0.85	H28A, H28B, H28C, H84A, H84B, H84C, H34A, H34B, H34C
		1.11	H48A, H48B, H65A, H65B, H82A, H82B
		2.91	H37B, H54B, H71B, H88B
		3.17	H88A, H98A, H98B, H37A, H54A, H71A
		4.15	H47, H81, H31

		4.54	H87, H18, H53
4.54	H87, H18, H53	1.11	H48A, H48B, H65A, H65B, H82A, H82B
		2.91	H37B, H54B, H71B, H88B
		3.16	H88A, H98A, H98B, H37A, H54A, H71A
		4.15	H47, H81, H31
4.30	H9, H26, H21	0.57	H33A, H33B, H33C, H23A, H23B, H23C, H51A, H51B, H51C, H68A, H68B, H68C, H5A, H5B, H5C
		0.81	H24A, H24B, H24C, H4A, H4B, H4C, H16A, H16B, H16C
		1.11	H48A, H48B, H65A, H65B, H82A, H82B
		2.02	H32, H27, H22
4.24	H12, H2, H64	0.79	H24A, H24B, H24C, H4A, H4B, H4C, H16A, H16B, H16C
		1.46	H13A, H13B
4.16	H47, H81, H31	0.58	H33A, H33B, H33C, H23A, H23B, H23C, H51A, H51B, H51C, H68A, H68B, H68C, H5A, H5B, H5C
		0.86	H28A, H28B, H28C, H84A, H84B, H84C, H34A, H34B, H34C
		1.11	H48A, H48B, H65A, H65B, H82A, H82B
		1.81	H3
		2.91	H37B, H54B, H71B, H88B
3.15	H88A, H98A, H98B, H37A, H54A, H71A	2.91	H37B, H54B, H71B, H88B
2.91	H37B, H54B, H71B, H88B	0.57	H33A, H33B, H33C, H23A, H23B, H23C, H51A, H51B, H51C, H68A, H68B, H68C, H5A, H5B, H5C
		1.11	H48A, H48B, H65A, H65B, H82A, H82B
2.01	H32, H27, H22	0.81	H24A, H24B, H24C, H4A, H4B, H4C, H16A, H16B, H16C
1.81	H3	0.57	H33A, H33B, H33C, H23A, H23B, H23C, H51A, H51B, H51C, H68A, H68B, H68C, H5A, H5B, H5C
1.56	H14	0.83	H28A, H28B, H28C, H84A, H84B, H84C, H34A, H34B, H34C
1.46	H13A, H13B	0.83	H28A, H28B, H28C, H84A, H84B, H84C, H34A, H34B, H34C
1.11	H48A, H48B, H65A, H65B, H82A, H82B	0.57	H33A, H33B, H33C, H23A, H23B, H23C, H51A, H51B, H51C, H68A, H68B, H68C, H5A, H5B, H5C
0.87	H28A, H28B, H28C, H84A, H84B, H84C,	0.57	H33A, H33B, H33C, H23A, H23B, H23C, H51A, H51B, H51C, H68A, H68B, H68C, H5A, H5B, H5C

	H34A, H34B, H34C

Table S10: Variation of NOE intensity and internuclear distance between two spatially close protons with different mixing time.

^{1}H Isotropic Chemical Shift (ppm)	^{1}H Isotropic Chemical Shift (ppm)	Intensity of the peak (at 0.1s mixing time)	Intensity of the peak (at 0.2s mixing time)	Intensity of the peak (at 0.3s mixing time)	Intensity of the peak (at 0.5s mixing time)	Intensity of the peak (at 0.7s mixing time)	Internuclear distance (according to 0.1s mixing time NOESY spectra)	Internuclear distance (according to 0.2s mixing time NOESY spectra)	Internuclear distance (according to 0.3s mixing time NOESY spectra)
10.76	0.57	2.309×10^9	4.123×10^9	7.321×10^9	1.034×10^{10}	1.312×10^{10}	2.84	3.03	3.33
	7.09	1.481×10^{10}	2.426×10^{10}	4.407×10^{10}	6.552×10^{10}	8.262×10^{10}	2.09	2.26	2.47
	7.31	3.539×10^9	6.556×10^9	1.175×10^{10}	1758×10^{10}	2.468×10^{10}	2.65	2.81	3.07
10.71	0.57	1.062×10^9	2.021×10^9	4.186×10^9	4.498×10^9	5.113×10^9	3.24	3.41	3.65
	7.09	6.764×10^9	1.149×10^{10}	2.377×10^{10}	2.524×10^{10}	2.885×10^{10}	2.38	2.55	2.73
	7.31	1.733×10^9	3.246×10^9	6.862×10^9	7.216×10^9	9.619×10^9	2.98	3.15	3.36
8.30	0.65	8.106×10^8	1.547×10^9	2.851×10^9	3.689×10^9	4.474×10^9	3.39	3.57	3.89
	1.20	1.834×10^9	3.363×10^9	5.547×10^9	8.209×10^9	1.019×10^{10}	2.96	3.14	3.48
	2.91	3.959×10^9	6.166×10^9	9.062×10^9	1.081×10^{10}	1.120×10^{10}	2.60	2.83	3.21
	3.23	1.433×10^9	2.769×10^9	4.763×10^9	7.691×10^9	8.506×10^9	3.08	3.24	3.57
	3.72	2.564×10^9	4.025×10^9	6.214×10^9	1.242×10^{10}	1.397×10^{10}	2.79	3.04	3.42
	4.17	1.022×10^{10}	1.616×10^{10}	2.489×10^{10}	3.025×10^{10}	3.120×10^{10}	2.22	2.41	2.71
	4.47	1.759×10^9	2.888×10^9	4.736×10^9	7.561×10^9	8.890×10^9	2.98	3.22	3.58
	7.94	2.731×10^9	4.109×10^9	5.931×10^9	9.267×10^9	1.031×10^{10}	2.77	3.03	3.44
8.21	0.58	2.224×10^9	3.301×10^9	7.289×10^9	1.075×10^{10}	1.347×10^{10}	2.86	3.15	3.33

	0.87	1.229×10^{9}	2.304×10^{9}	3.741×10^{9}	6.258×10^{9}	7.715×10^{9}	3.160	3.34	3.72
	1.11	3.932×10^{9}	5.845×10^{9}	1.222×10^{10}	1.450×10^{10}	1.675×10^{10}	2.60	2.86	3.05
	2.91	8.112×10^{9}	9.577×10^{9}	1.842×10^{10}	1.982×10^{10}	2.045×10^{10}	2.31	2.63	2.85
	3.17	3.862×10^{9}	5.396×10^{9}	1.243×10^{10}	1.575×10^{10}	1.757×10^{10}	2.61	2.90	3.04
	4.15	1.513×10^{10}	2.222×10^{10}	4.350×10^{10}	4.243×10^{10}	3.349×10^{10}	2.08	2.29	2.47
	4.54	4.648×10^{9}	7.441×10^{9}	1.291×10^{10}	1.570×10^{10}	1.794×10^{10}	2.53	2.75	3.03
	7.09	1.455×10^{9}	2.445×10^{9}	4.281×10^{9}	6.069×10^{9}	7.437×10^{9}	3.07	3.31	3.64
8.13	0.59	2.129×10^{9}	4.112×10^{9}	7.432×10^{9}	1.208×10^{10}	1.460×10^{10}	2.88	3.03	3.32
	0.83	1.005×10^{9}	1.936×10^{9}	3.434×10^{9}	5.348×10^{9}	7.731×10^{9}	3.27	3.44	3.77
	1.20	1.895×10^{9}	3.426×10^{9}	5.996×10^{9}	8.864×10^{9}	8.763×10^{9}	2.94	3.13	3.44
	1.46	3.956×10^{9}	6.519×10^{9}	1.034×10^{10}	1.376×10^{10}	1.014×10^{10}	2.60	2.81	3.14
	1.81	2.203×10^{9}	3.684×10^{9}	5.953×10^{9}	8.226×10^{9}	8.729×10^{9}	2.87	3.09	3.44
	2.91	4.003×10^{9}	5.600×10^{9}	8.322×10^{9}	1.035×10^{10}	9.984×10^{9}	2.59	2.88	3.26
	3.12	1.814×10^{9}	3.425×10^{9}	6.201×10^{9}	8.642×10^{9}	9.344×10^{9}	2.96	2.13	3.42
	4.22	9.227×10^{9}	1.423×10^{10}	2.403×10^{10}	2.965×10^{10}	2.587×10^{10}	2.26	2.47	2.73
	4.56	2.350×10^{9}	3.707×10^{9}	6.157×10^{9}	8.524×10^{9}	8.968×10^{9}	2.84	3.09	3.42
8.03	0.59	5.385×10^{8}	1.136×10^{9}	2.310×10^{9}	3.929×10^{9}	4.429×10^{9}	3.63	3.76	4.03
	0.97	1.261×10^{9}	1.991×10^{9}	3.886×10^{9}	5.061×10^{9}	4.955×10^{9}	3.15	3.42	3.70
	1.20	5.389×10^{9}	8.965×10^{9}	1.619×10^{10}	1.998×10^{10}	1.747×10^{10}	2.47	2.66	2.91
	2.91	9.719×10^{8}	1.893×10^{9}	4.176×10^{9}	5.372×10^{9}	6.631×10^{9}	3.29	3.45	3.65
	3.15	1.285×10^{9}	2.193×10^{9}	4.645×10^{9}	5.675×10^{9}	6.865×10^{9}	3.14	3.37	3.59
	4.15	2.722×10^{9}	4.283×10^{9}	8.214×10^{9}	9.382×10^{9}	1.038×10^{10}	2.77	3.01	3.26
	4.56	5.900×10^{9}	9.002×10^{10}	1.833×10^{10}	2.031×10^{10}	1.826×10^{10}	2.43	1.81	2.85
7.93	0.58	2.102×10^{9}	4.808×10^{9}	8.633×10^{9}	1.342×10^{10}	1.311×10^{10}	2.89	2.95	3.24

	0.80	7.528×10^{9}	1.226×10^{10}	1.746×10^{10}	2.856×10^{10}	2.781×10^{10}	2.34	2.53	2.88
	1.20	1.304×10^{10}	2.156×10^{10}	3.425×10^{10}	4.126×10^{10}	4.297×10^{10}	2.13	2.30	2.57
	1.46	8.542×10^{8}	1.824×10^{9}	5.399×10^{9}	7.180×10^{9}	6.821×10^{9}	3.36	3.47	3.50
	2.01	4.430×10^{9}	7.187×10^{9}	1.170×10^{10}	1.438×10^{10}	1.560×10^{10}	2.55	2.76	3.08
	2.92	3.214×10^{9}	5.920×10^{9}	1.095×10^{10}	1.640×10^{10}	1.138×10^{10}	2.69	2.85	3.11
	3.17	6.354×10^{9}	1.088×10^{10}	1.933×10^{10}	2.790×10^{10}	1.741×10^{10}	2.40	2.58	2.83
	4.29	1.298×10^{10}	2.259×10^{10}	3.466×10^{10}	4.364×10^{10}	4.610×10^{10}	2.13	2.28	2.57
	4.55	1.422×10^{10}	2.201×10^{10}	3.477×10^{10}	4.058×10^{10}	3.146×10^{10}	2.10	2.29	2.57
	7.77	5.140×10^{9}	7.397×10^{9}	9.109×10^{9}	1.021×10^{10}	1.010×10^{10}	2.49	2.75	3.21
	7.74	5.812×10^{9}	7.854×10^{9}	1.141×10^{10}	1.393×10^{10}	1.418×10^{10}	2.44	2.72	3.09
7.78	0.59	4.598×10^{9}	7.368×10^{9}	1.183×10^{10}	1.540×10^{10}	1.683×10^{10}	2.54	2.75	3.07
	0.78	2.272×10^{9}	4.646×10^{9}	7.190×10^{9}	1.129×10^{10}	1.397×10^{10}	2.85	2.97	3.34
	1.81	1.948×10^{9}	3.140×10^{9}	5.127×10^{9}	6.609×10^{9}	6.776×10^{9}	2.93	3.17	3.53
	2.01	2.431×10^{9}	4.639×10^{9}	6.794×10^{9}	9.484×10^{9}	1.029×10^{10}	2.82	2.97	3.37
	4.29	8.335×10^{9}	1.265×10^{10}	2.128×10^{10}	2.581×10^{10}	2.573×10^{10}	2.30	2.51	2.78
7.73	0.80	4.591×10^{9}	7.034×10^{9}	1.189×10^{10}	1.245×10^{10}	1.815×10^{10}	2.54	2.77	3.07
	1.20	2.433×10^{9}	3.761×10^{9}	4.121×10^{9}	9.926×10^{9}	7.909×10^{9}	2.82	3.08	3.66
	2.01	1.967×10^{9}	3.186×10^{9}	5.262×10^{9}	7.125×10^{9}	7.630×10^{9}	2.92	3.16	3.51
	4.31	9.429×10^{9}	1.386×10^{10}	2.430×10^{10}	3.205×10^{10}	3.304×10^{10}	2.25	2.48	2.72
7.57	2.91	9.551×10^{8}	1.861×10^{9}	5.221×10^{9}	6.994×10^{9}	8.743×10^{9}	3.30	3.46	3.52
	3.18	1.477×10^{9}	4.103×10^{9}	6.412×10^{9}	9.010×10^{9}	1.010×10^{10}	3.06	3.03	3.40
	4.53	2.188×10^{9}	3.864×10^{9}	6.729×10^{9}	8.955×10^{9}	1.015×10^{10}	2.87	3.06	3.37
	6.95	2.250×10^{9}	7.187×10^{9}	2.195×10^{10}	2.523×10^{10}	2.902×10^{10}	2.86	2.76	2.77
7.54	0.57	1.153×10^{9}	2.367×10^{9}	4.016×10^{9}	6.492×10^{9}	8.241×10^{9}	3.19	3.32	3.68
	2.91	$2.093\times$	3.902	6.764	1.071	1.332	2.89	3.06	3.37

		10^9	$\times 10^9$	$\times 10^9$	$\times 10^{10}$	$\times 10^{10}$			
	3.14	2.851×10^9	2.907×10^9	7.771×10^9	1.150×10^{10}	1.345×10^{10}	2.75	3.21	3.29
	4.51	3.296×10^9	4.572×10^9	9.333×10^9	1.326×10^{10}	1.609×10^{10}	2.68	2.98	3.19
	6.95	6.972×10^9	9.507×10^9	1.880×10^{10}	3.011×10^{10}	3.590×10^{10}	2.37	2.64	2.84
7.29	0.57	1.122×10^9	2.090×10^9	3.435×10^9	5.086×10^9	6.466×10^9	3.21	3.39	3.77
	7.03	6.252×10^9	1.635×10^{10}	5.068×10^{10}	4.614×10^{10}	6.567×10^{10}	2.41	2.41	2.41
7.08	0.57	3.455×10^9	6.319×10^9	1.233×10^{10}	1.748×10^{10}	2.217×10^{10}	2.66	2.82	3.05
	0.85	1.104×10^9	2.074×10^9	4.724×10^9	6.786×10^9	8.773×10^9	3.22	3.40	3.58
	1.20	1.553×10^9	2.331×10^9	5.279×10^9	7.702×10^9	1.029×10^{10}	3.04	3.33	3.51
	2.91	5.386×10^9	9.197×10^9	1.445×10^{10}	1.965×10^{10}	2.251×10^{10}	2.47	2.65	2.97
	3.17	2.651×10^9	3.332×10^9	9.220×10^9	1.198×10^{10}	1.657×10^{10}	2.78	3.14	3.20
	4.15	9.080×10^8	2.018×10^9	4.019×10^9	6.814×10^9	8.626×10^9	3.32	3.41	3.68
	4.54	2.475×10^9	4.488×10^9	6.774×10^9	1.351×10^{10}	1.645×10^{10}	2.81	2.99	3.37
4.54	1.20	1.067×10^9	2.201×10^9	3.915×10^9	7.358×10^9	9.142×10^9	3.23	3.37	3.69
	2.91	5.791×10^9	8.646×10^9	1.302×10^{10}	1.864×10^{10}	2.110×10^{10}	2.44	2.68	3.02
	3.16	5.072×10^9	1.003×10^{10}	1.432×10^{10}	1.877×10^{10}	2.147×10^{10}	2.49	2.61	2.97
	4.15	1.227×10^9	2.402×10^9	4.084×10^9	7.461×10^9	9.807×10^9	3.16	3.32	3.67
4.30	0.57	1.087×10^9	1.708×10^9	4.240×10^9	7.284×10^9	6.133×10^9	3.22	3.51	3.64
	0.81	8.797×10^9	1.554×10^{10}	2.579×10^{10}	4.011×10^{10}	3.972×10^9	2.28	2.43	2.69
	1.20	4.819×10^9	8.485×10^9	1.661×10^{10}	2.104×10^{10}	2.358×10^{10}	2.52	2.69	2.90
	2.02	5.799×10^9	1.015×10^{10}	1.896×10^{10}	2.048×10^{10}	2.336×10^{10}	2.44	2.61	2.83
4.24	0.79	2.934×10^9	4.903×10^9	7.162×10^9	1.178×10^{10}	1.375×10^{10}	2.73	2.94	3.34
	1.46	4.390×10^9	6.016×10^9	8.776×10^9	1.358×10^{10}	1.528×10^{10}	2.56	2.84	3.23
4.16	0.58	1.153×10^{10}	1.931×10^{10}	3.106×10^{10}	3.966×10^{10}	4.371×10^{10}	2.18	2.34	2.61
	0.86	1.617×10^9	3.716×10^9	5.923×10^9	8.436×10^9	9.990×10^9	3.02	3.08	3.45

	1.20	8.656×10^{9}	1.509×10^{10}	2.176×10^{10}	2.793×10^{10}	2.898×10^{10}	2.28	2.44	2.77
	1.81	3.086×10^{9}	6.889×10^{9}	7.772×10^{9}	1.361×10^{10}	1.435×10^{10}	2.71	2.78	3.29
	2.91	1.277×10^{9}	2.796×10^{9}	5.511×10^{9}	9.366×10^{9}	1.213×10^{10}	3.14	3.23	3.49
3.15	0.57	9.199×10^{8}	1.712×10^{9}	2.772×10^{9}	4.337×10^{9}	5.671×10^{9}	3.32	3.51	3.91
	1.20	1089×10^{9}	1.889×10^{9}	3.217×10^{9}	4.895×10^{9}	5.710×10^{9}	3.22	3.45	3.81
	2.91	4.453×10^{10}	4.514×10^{10}	4.862×10^{10}	4.530×10^{10}	4.229×10^{10}	1.74	2.03	2.43
2.91	0.57	1.453×10^{9}	2.019×10^{9}	4.780×10^{9}	7.526×10^{9}	8.544×10^{9}	3.07	3.41	3.57
	1.20	1.435×10^{9}	2.645×10^{9}	4.235×10^{9}	6.531×10^{9}	8.530×10^{9}	3.08	3.26	3.64
2.01	0.81	1512×10^{10}	2.227×10^{10}	3.724×10^{10}	4.707×10^{10}	4.752×10^{10}	2.08	2.29	2.54
1.81	0.57	6.235×10^{9}	1.003×10^{10}	1.824×10^{10}	2.255×10^{10}	2.245×10^{10}	2.41	2.61	2.86
1.56	0.83	2.970×10^{9}	4.196×10^{9}	7.450×10^{9}	8.955×10^{9}	1.060×10^{10}	2.73	3.02	3.32
1.46	0.83	4.406×10^{9}	7.526×10^{9}	1.258×10^{10}	1.578×10^{10}	1.617×10^{10}	2.55	2.74	3.04
1.20	0.57	8.454×10^{9}	1.288×10^{10}	2.063×10^{10}	2.765×10^{10}	2.587×10^{10}	2.29	2.51	2.80
0.87	0.57	1.043×10^{10}	1.608×10^{10}	2.152×10^{10}	2.606×10^{10}	2.643×10^{10}	2.21	2.42	2.78

Table S11: Assignment of ^{13}C CP-MAS SSNMR Spectrum for Gramicidin A

Position of Isotropic Chemical Shift (ppm)	Carbon Nuclei
173.8	C6- Carbonyl group carbon of L-Valine (1)
	C8-Carbonyl group carbon of D-Glycine
	C11-Carbonyl group carbon of L-Alanine (1)
	C17- Carbonyl group carbon of D-Leucine (1)
	C20-Carbonyl group carbon of L-Alanine (2)
	C25-Carbonyl group carbon of D-Valine (2)
	C30-Carbonyl group carbon of L-Valine (3)
	C35-Carbonyl group carbon of D-Valine (4)
	C46-Carbonyl group carbon of L-Tryptophan (1)
	C52-Carbonyl group carbon of D-Leucine (2)
	C63-Carbonyl group carbon of L-Tryptophan (2)
	C69-Carbonyl group carbon of D-Leucine (3)
	C80-Carbonyl group carbon of L-Tryptophan (3)

	C86-Carbonyl group carbon of D-Leucine (4)
	C97-Carbonyl group carbon of L-Tryptophan (4)
165.0	C1- Carbon nuclei of formyl group
137.8	C40 - Carbon nuclei residing on Indole group of L-Tryptophan (1)
	C57 -Carbon nuclei residing on Indole group of L-Tryptophan (2)
	C74 -Carbon nuclei residing on Indole group of L-Tryptophan (3)
	C91 -Carbon nuclei residing on Indole group of L-Tryptophan (4)
129.4	C45 -Carbon nuclei residing on Indole group of L-Tryptophan (1)
	C62 -Carbon nuclei residing on Indole group of L-Tryptophan (2)
	C79 -Carbon nuclei residing on Indole group of L-Tryptophan (3)
	C96 -Carbon nuclei residing on Indole group of L-Tryptophan (4)
123.0	C39-Carbon nuclei residing on Indole group of L-Tryptophan (1)
	C56-Carbon nuclei residing on Indole group of L-Tryptophan (2)
	C73-Carbon nuclei residing on Indole group of L-Tryptophan (3)
	C90-Carbon nuclei residing on Indole group of L-Tryptophan (4)
121.9	C42, C43, C44-Carbon nuclei residing on Indole group of L-Tryptophan (1)
	C59, C60, C61 -Carbon nuclei residing on Indole group of L-Tryptophan (2)
	C76, C77, C78- Carbon nuclei residing on Indole group of L-Tryptophan (3)
	C93, C94, C95- Carbon nuclei residing on Indole group of L-Tryptophan (4)
112.6	C38, C41- Carbon nuclei residing on Indole group of L-Tryptophan (1)
	C55, C58- Carbon nuclei residing on Indole group of L-Tryptophan (2)
	C72,C75- Carbon nuclei residing on Indole group of L-Tryptophan (3)
	C89,C92- Carbon nuclei residing on Indole group of L-Tryptophan (4)
57.9	C2- carbon nuclei residing on the amino acid L-Valine (1)
	C12- carbon nuclei residing on the amino acid D-Leucine (1)
	C21- carbon nuclei residing on the amino acid D-Valine (2)
	C26- carbon nuclei residing on the amino acid L-Valine (3)
	C31- carbon nuclei residing on the amino acid D-Valine (4)
	C36 - carbon nuclei residing on the amino acid L-Tryptophan (1)
	C47- carbon nuclei residing on the amino acid D-Leucine(2)
	C53 - carbon nuclei residing on the amino acid L-Tryptophan (2)
	C64 -carbon nuclei residing on the amino acid D-Leucine (3)
	C70 - carbon nuclei residing on the amino acid L-Tryptophan (3)
	C81 - carbon nuclei residing on the amino acid D-Leucine (4)
	C87 - carbon nuclei residing on the amino acid L-Tryptophan (4)
	C99 - carbon nuclei residing on the molecular moiety ethanolamine ($NHCH_2CH_2OH$)
54.1	C9-carbon nuclei residing on the amino acid L-Alanine (1)
	C18-carbon nuclei residing on the amino acid L-Alanine (2)
43.7	C7- carbon nuclei residing on the amino acid D-Glycine
	C13- carbon nuclei residing on the amino acid D-Leucine (1)
	C48- carbon nuclei residing on the amino acid D-Leucine (2)
	C65-carbon nuclei residing on the amino acid D-Leucine (3)
	C82- carbon nuclei residing on the amino acid D-Leucine (4)
	C98- carbon nuclei residing on the molecular moiety ethanolamine ($NHCH_2CH_2OH$)
33.0	C22- carbon nuclei residing on the amino acid D-Valine (2)
	C27 - carbon nuclei residing on the amino acid L-Valine (3)

	C32 - carbon nuclei residing on the amino acid D- Valine (4)
25.7	C37 - carbon nuclei residing on the amino acid L-Tryptophan (1)
	C54- carbon nuclei residing on the amino acid L-Tryptophan (2)
	C71- carbon nuclei residing on the amino acid L-Tryptophan (3)
	C88 - carbon nuclei residing on the amino acid L-Tryptophan (4)
24.5	C14- carbon nuclei residing on the amino acid D-Leucine (1)
	C49-carbon nuclei residing on the amino acid D-Leucine (2)
	C66- carbon nuclei residing on the amino acid D-Leucine (3)
	C83-carbon nuclei residing on the amino acid D-Leucine (4)
21.3	C15, C16 - methyl group carbon nuclei residing on the amino acid D-Leucine (1)
	C50, C51 - methyl group carbon nuclei residing on the amino acid D-Leucine (2)
	C67, C68 - methyl group carbon nuclei residing on the amino acid D-Leucine (3)
	C84, C85 - methyl group carbon nuclei residing on the amino acid D-Leucine (4)
18.5	C4, C5 – methyl group carbon nuclei residing on the amino acid L-Valine(1)
	C10- methyl group carbon nuclei residing on the amino acid D-Glycine
	C19 – methyl group carbon nuclei residing on the amino acid L-Alanine (2)
	C23, C24 – methyl group carbon nuclei residing on the amino acid D-Valine (2)
	C28, C29 – methyl group carbon nuclei residing on the amino acid L-Valine (3)
	C33, C34 – methyl group carbon nuclei residing on the amino acid D-Valine (4)

The Principal Components of the CSA Parameters

Solid-state NMR spectroscopy is a powerful technique that provides detailed information about the structure and dynamics of molecules at atomic-scale resolution. In such experiments, several types of nuclear spin interactions are probed and manipulated. These include: (i) magnetic shielding interactions caused by surrounding electrons, which lead to chemical shifts; (ii) through-space dipole–dipole couplings and through-bond indirect dipole–dipole couplings between neighboring nuclear spins; and (iii) quadrupolar interactions between nuclei possessing a quadrupole moment. All these spin interactions are local in nature. The magnetic field experienced by a nucleus is not identical to the externally applied magnetic field (^{B_0}). The motion of surrounding electrons in response to ^{B_0} generates a secondary magnetic field at the nucleus, which partially shields or deshields it. The magnitude of this secondary field is proportional to ^{B_0}, and the effective magnetic field experienced by the nucleus can be expressed as $B_{eff} = (B_0 \pm \sigma B_0)$, where σ is the magnetic shielding tensor.[38-42] The value of σ depends on the molecular orientation relative to ^{B_0}. Consequently, the resonance frequency of a nucleus varies with its local chemical and electronic environment. The magnetic shielding tensor has nine components and describes how the local magnetic field at the nucleus changes due to electron– magnetic field interactions. Depending on these interactions, the nucleus may experience shielding or deshielding effects. In the principal axis system (PAS), only the diagonal components of the tensor $^{\sigma_{11}}$, $^{\sigma_{22}}$, and $^{\sigma_{33}}$remain non-zero. These values vary with molecular orientation according to Ramsey's shielding theory.[43,44]

$$\sigma_{33} = \frac{e^2}{2m}\left\langle 0\left|\frac{x^2 + y^2}{r^3}\right|0\right\rangle - \left(\frac{e\hbar}{2m}\right)^2 \sum_n \left\{\frac{\langle 0|L_z|n\rangle\left\langle n\left|\frac{2L_z}{r^3}\right|0\right\rangle}{(E_n - E_0)} + \frac{\left\langle 0\left|\frac{2L_z}{r^3}\right|n\right\rangle\langle n|L_z|0\rangle}{(E_n - E_0)}\right\} \quad (5)$$

$$\sigma_{11} = \frac{e^2}{2m}\left\langle 0\left|\frac{y^2 + z^2}{r^3}\right|0\right\rangle - \left(\frac{e\hbar}{2m}\right)^2 \sum_n \left\{\frac{\langle 0|L_x|n\rangle\left\langle n\left|\frac{2L_x}{r^3}\right|0\right\rangle}{(E_n - E_0)} + \frac{\left\langle 0\left|\frac{2L_x}{r^3}\right|n\right\rangle\langle n|L_x|0\rangle}{(E_n - E_0)}\right\} \quad (6)$$

$$\sigma_{22} = \frac{e^2}{2m}\left\langle 0\left|\frac{x^2 + z^2}{r^3}\right|0\right\rangle - \left(\frac{e\hbar}{2m}\right)^2 \sum_n \left\{\frac{\langle 0|L_y|n\rangle\left\langle n\left|\frac{2L_y}{r^3}\right|0\right\rangle}{(E_n - E_0)} + \frac{\left\langle 0\left|\frac{2L_y}{r^3}\right|n\right\rangle\langle n|L_y|0\rangle}{(E_n - E_0)}\right\} \quad (7)$$

The components L_x, L_y, and L_z represent the x, y, and z components of angular momentum, respectively, which are related to the electron cloud distribution and molecular rotational motion. The principal components of the magnetic shielding tensor, σ_{11}, σ_{22}, and σ_{33}, arise from two main contributions: diamagnetic and paramagnetic terms. The diamagnetic term originates from the spherically symmetric electron distribution in the ground electronic state, while the paramagnetic term results from distortions in this spherical symmetry, typically due to the involvement of excited electronic states. In simpler terms, the paramagnetic contribution becomes significant when there is an asymmetric distribution of p- and d-orbital electrons near the nucleus, whereas it is negligible for s-orbital electrons, which have zero orbital angular momentum. These two contributions vary for the same nucleus depending on its local chemical and electronic environment. Consequently, the chemical shift depends on both molecular orientation and the surrounding electronic structure. Therefore, the chemical shift anisotropy (CSA) patterns observed for crystallographically distinct carbon sites in gramicidin A provide insights into molecular motions and alignment relative to the local magnetic field. Additionally, CSA patterns are characteristic of specific nuclei and functional groups, making them useful for chemical identification and resonance assignment in solid-state NMR studies.

NMR experiments do not measure magnetic shielding directly, instead it measures the chemical shift, δ, the change of the resonance frequency of a nucleus. The relation between the chemical shift and magnetic shielding is given by[42]

$$\delta_{i=} \frac{\sigma_{ref} - \sigma_i}{1 - \sigma_{ref}}$$

σ_{ref} is the shielding of the reference compound used in the NMR experiment, and σ_i is the shielding of the measured compound.

Reference:

1. Levitt, M. H.; Madhu P. K.; Hughes C. E. Cogwheel phase cycling. *Journal of Magnetic Resonance* **2002**, *155*, 300-306.
2. Ivchenko, N.; Hughes, C. E.; Levitt, M. H. Application of cogwheel phase cycling to sideband manipulation experiments in solid-state NMR. *Journal of Magnetic Resonance* **2003**, *164*, 286–293.
3. Ghosh, M.; Sadhukhan, S.; Dey, K. K. Elucidating the internal structure and dynamics of α-chitin by 2DPASS-MAS-NMR and spin-lattice relaxation measurements. *Solid State Nuclear Magnetic Resonance* **2019**, *97*, 7-16.
4. Herzfeld, J.; Berger, A. E. Sideband Intensities in NMR Spectra of Samples Spinning at the Magic Angle. *Journal of Chemical Physics* **1980**, *73*, 6021-6030.
5. Tycko, R.; Dabbagh, G.; Mirau, P. A. Determination of chemical shift anisotropy lineshapes in a two-dimensional magic angle spinning NMR experiment. *Journal of Magnetic Resonance* **1989**, *85*, 265-274.
6. Liu, S. F.; Mao, J. D.; Schmidt-Rohr, K. A robust technique for two-dimensional separation of undistorted chemical shift anisotropy powder patterns in magic angle spinning NMR. *Journal of Magnetic Resonance* **2002**, *155*, 15-28.
7. Chan, J. C. C.; R. Tycko, R. Recoupling of chemical shift anisotropies in solid state NMR under high speed magic angle spinning and in uniformly ^{13}C labelled systems. *Journal of Chemical Physics* **2003**, *118*, 8378-8389.
8. G. Hou, L. Byeon In-Ja, J. Ahn, A. M. Gronenborn, and T. Polenova, Recoupling of chemical shift anisotropy by R-symmetry sequences in magic angle spinning NMR spectroscopy. *Journal of Chemical Physics* **2012**, *137*,134201-134210.
9. Bax, AD; Szeverenyi, N. M.; Maciel, G. E. Chemical shift anisotropy in powdered solids studied by 2D FT NMR with flipping of the spinning axis. *Journal of Magnetic Resonance* **1983**, *55*, 494-497.
10. Bax, AD; Szeverenyi, N. M.; Maciel, G. E. Correlation of isotropic shifts and chemical shift anisotropies by two-dimensional Fourier-transform magic angle hopping NMR spectroscopy. *Journal of Magnetic Resonance* **1983**, *52*, 147-152.
11. Bax, AD; Szeverenyi, N. M.; Maciel, G. E. Chemical shift anisotropy in powdered solids studied by 2D FT CP/MAS NMR. *Journal of Magnetic Resonance* **1983**, *51*, 400-408.
12. Gan, Z. High-resolution chemical shift and chemical shift anisotropy correlation in solids using slow magic angle spinning. *Journal of American Chemical Society* **1992**, *114*, 8307-8309.
13. Ghosh, M.; Sadhukhan, S.; Dey, K. K. Elucidating the internal structure and dynamics of α-chitin by 2DPASS-MAS-NMR and spin-lattice relaxation measurements. *Solid State Nuclear Magnetic Resonance* **2019**, *97*, 7-16.
14. Ghosh, M.; Prajapati, B. P.; Kango, N.; Dey, K. K. A comprehensive and comparative study of the internal structure and dynamics of natural β-keratin and regenerated β-keratin by solid state NMR spectroscopy. *Solid State Nuclear Magnetic Resonance* **2019**, *101*, 1-11.
15. Ghosh, M.; Kango, N.; Dey, K. K. Investigation of the internal structure and dynamics of cellulose by ^{13}C-NMR relaxometry and 2DPASS-MAS-NMR measurements. *Journal of Biomolecular NMR* **2019**, *73*, 601-616.
16. Dey, K. K.; Ghosh, M. Understanding the effect of deacetylation on chitin by measuring chemical shift anisotropy tensor and spin lattice relaxation time, *Chemical Physics Letters* **, 2020**, *738*, 136782.

17. Dey, K. K.; Gayen, S.; Ghosh, M. Structure and dynamics of sodium alginate as elucidated by chemical shift anisotropy and site-specific spin–lattice relaxation time measurements. *European Biophysics Journal* **2021**, *50*(7), 963-977.
18. Mandal, I.; Keshri, S. R.; Lodhi, L.; Dey, K. K.; Ghosh, M.; Ghosh, A.; Allu, A. R. Correlation of structure and ionic-conductivity in phosphate glass using MAS-NMR and impedance spectroscopy: Influence of sodium salt. *Physical Review Materials* **2022**, *6*, 115403.
19. Bhowal, R.; Balaraman, A.; Ghosh, M.; Dutta, S.; Dey, K. K.; Chopra, D. Probing Atomistic Behavior to Unravel Dielectric Phenomena in Charge Transfer Cocrystals. *Journal of the American Chemical Society* **2021**, *143*, 1024-1037.
20. Wang, N.; Tang, D.; Shu, J. An improved scheme for measuring ^{13}C spin-lattice relaxation time: targeting systems with marked difference in phase mobility or proton density, *Polymer Testing*, **2019**, *77*, 105920.
21. Rance, M.; Sørensen, O. W.; Bodenhausen, G.; Wagner, G.; Ernst, R. R.; Wüthrich, K. Improved spectral resolution in homo- and heteronuclear two-dimensional correlation spectroscopy by double quantum filtering. *Biochemical and Biophysical Research Communications* **1983,** *117* (2), 479–485. DOI: 10.1016/0006-291X(83)90491-8.
22. Hurd, R. E. Gradient-enhanced spectroscopy. *Journal of Magnetic Resonance (1969)* **1990,** *87* (3), 638–642. DOI: 10.1016/0022-2364(90)90350-S.
23. Bodenhausen, G. and Ruben, D. J. (1980). "Sensitivity optimization in two-dimensional multiple-quantum NMR spectroscopy". *Chemical Physics Letters*, 69(1): 185-189.
24. Kupče, Ē. and Freeman, R. (2007). "Adiabatic pulses for inversion and refocusing in INEPT-based experiments". *Journal of Magnetic Resonance*, 187(2): 288-293.
25. Bax, A., and G. E. Martin. "Gradient-selected two-dimensional heteronuclear multiple-bond correlation spectroscopy." *Journal of the American Chemical Society* 113.11 (1991): 4370-4371.
26. Martin, G. E., and R. C. Crouch. "Inverse-detected long-range heteronuclear shift correlation spectroscopy: a review." *Journal of Natural Products* 54.1 (1991): 1-33.
27. Kovacs, H., D. Moskau, and M. Spraul. "Gradient selection in high-resolution NMR spectroscopy." *Progress in Nuclear Magnetic Resonance Spectroscopy* 46.2 (2005): 131-155
28. Jeener, J.; Meier, B. H.; Bachmann, P.; Ernst, R. R. "Investigation of exchange processes by two-dimensional NMR spectroscopy". *J. Chem. Phys.* **1979**, 71 (11), 4546-4553.
29. Wagner, R.; Berger, S. "Gradient-Selected NOESY—A Fourfold Reduction of the Measurement Time for the NOESY Experiment." *Journal of Magnetic Resonance, Series A* **1996**, *123* (1), 119-121.
30. Hawkes, G. H.; Lian, L. Y.; Randall, E. W.; Sales, K. D.; Curzon, E. H. The conformation of gramicidin A in dimethylsulphoxide solution: A full analysis of the one-and two-dimensional ^{1}H, ^{13}C, and ^{15}N nuclear-magnetic-resonance spectra. *Eur. J. Biochem.*, **1987**, *166*(2), 437-445.
31. Dixon, W. T. Spinning-sideband-free and spinning-sideband only NMR spectra in spinning samples, J. Chem. Phys., **1982**, *77*, 1800−1809.

32. Antzutkin, O. N.; Shekar, S. C.; Levitt, M. H. Two-dimensional sideband separation in magic angle spinning NMR, *J. Magn. Reson.* A, **1995**, *115*, 7−19.
33. Dey, K. K.; Ghosh, M. Understanding the Effect of an Anionic Side-Chain on the Nuclear Spin Dynamics of a Polysaccharide, *Cellulose*, **2022**, *29*, 1381–1392.
34. Lodhi, L.; Yadav, J. P.; Yamazaki, T.; Duong, N. T.; Poojary, S. L.; Dey, K. K.; Nishiyama, Y.; Ghosh, M. NMR Crystallographic Approach to Study the Variation of the Dynamics of Quinine and its Quasienantimer Quinidine, *J. Phys. Chem.* C, **2022**, *126*, 17291-17305.
35. Yadav, J. P.; Lodhi, L.; Fatma, T.; Dey, K. K.; Ghosh, M. Investigation of the Influence of Various Functional Groups on the Dynamics of Glucocorticoids. *ACS Omega*, **2022**, *7*, 43190-43209.
36. Dey, K. K.; Deshmukh, M. M.; Ghosh, M. A Description of the Local Structure and Dynamics of Ketoconazole Molecule by Solid-State NMR Measurements and DFT Calculations: Proposition for NMR Crystallography, *Chem. Select*, **2021**, *6*, 10208-10220.
37. Torchia, D. A. The measurement of proton-enhanced carbon-13 T1 values by method which suppresses artifacts, *J. Magn. Reson.*, **1978**, *30*, 613-616.
38. Saito, H.; Ando I.; Ramamoorthy A. Chemical Shift tensor-the heart of NMR: Insight into biological aspects of proteins. *Progress in Nuclear Magnetic Resonance Spectroscopy*, **2010**, 57, 181-228.
39. Ying, J.; Grishaev, A.; Bryce, D. L.; Bax AD. Chemical Shift Tensors of Protonated Base Carbons in Helical RNA and DNA from NMR Relaxation and Liquid Crystal Measurements. *Journal of the American Chemical Society*, **2006**, 128, 11443-11454.
40. Wei, Y.; Lee, D. K.; Ramamoorthy A. Solid-state ^{13}C NMR Chemical Shift Anisotropy Tensors of polypeptides. *Journal of the American Chemical Society*, **2001**, 123, 6118-6126.
41. Orendt, A.M. ; Facelli, J.C. Solid state effects on NMR chemical shifts. *Annual Report NMR Spectroscopy*, **2007**, 62, 115-178.
42. Harris, R. K.; Wasylishen, R. E.; Duer, M. J. NMR Crystallography, Wiley 2009
43. Ramsey, N.F. Magnetic Shielding of Nuclei in Molecules. *Physical Review*, **1950**, 78, 699-703.
44. Ramsey, N.F. Chemical effects in nuclear magnetic resonance and in diamagnetic susceptibility. *Physical Review*, **1952**, 86, 243-246.
45.